DEFORMATION AND UPLIFT OF NORTH AMERICA IN THE CENOZOIC ERA

by
Dr. Peter Bird
Department of Earth and Space Sciences
University of California
Los Angeles, CA 90024

January 10, 1991

Now published as:

Bird, Peter (1992) "Deformation and uplift of North America in the Cenozoic era", in K. R. Billingsley, H. U. Brown, III, and E. Derohanes (eds.), Scientific Excellence in Supercomputing: the 1990 IBM contest prize papers, Baldwin Press, Athens, Georgia, 1992, v. 1, pp. 67-105; v. 2, 2 end-plates.

ABSTRACT

Progress in science requires experiments, and the only way to experiment with continental deformation is to numerically solve the governing equations. A realistic model of practical computational speed has been achieved by a combination of multi-layer 2-D finite element methods (solving stress-equilibrium in the lithosphere), analytic methods (determining thickness and temperature changes) and finite difference methods (predicting lateral extrusion of soft lower crust). These models incorporate realistic frictional/creeping rheology, compositional layering of the lithosphere, possible detachment on horizontal planes, and feedback between deformation and heat conduction.

In the method's first application, 18 simulations were performed of the tectonic history of North America during the last 85 million years, when the Rocky Mountains formed (by compression), the Great Basin crust was thinned (by extension), and the continental interior was uplifted (mechanism unknown). The boundary conditions were obtained from published rigid-plate kinematic models of the ocean basins, and included horizontal subduction of the Farallon and/or Kula plates. In every model, shear traction from horizontal subduction caused detachment and eastward transport of the mantle layer of North American lithosphere. Next, the crustal roots of the Mesozoic coastal cordillera were sheared off and transported toward the Rocky Mountain foreland. Meanwhile, the resulting horizontal compressive stress caused crustal shortening (and further thickening) in the Rocky Mountain states. By systematic adjustment of the assumed rheological constants, strains of the correct magnitude in the correct states and epochs were "predicted." In the last 30 million years of each simulation, horizontal subduction ceased, and strike-slip faulting began along the southwest Pacific margin. Each model showed some approximation of the actual extension of the Great Basin, plus the large clockwise rotations of southwestern California that have been recently documented.

Principal scientific results to date include (1) verifying the hypothesis that horizontal subduction caused the shortening of the Rocky Mountains; (2) extending the hypothesis to explain the mechanism of continental uplift; (3) modeling the mechanism for heating and weakening of Great Basin crust, and (4) determining an in-situ rheology for the North American plate.

The modeling program was developed on an IBM 3090/VF, and achieves up to 50% of its CPU time in vector mode; execution times are 6-8 hours with vectorization. Accessory programs assist the preparation of plate reconstructions, editing of initial-condition files, and preparation of color contour maps of the output through time; these programs also require the 3090's speed, but provide graphics output on 3179 terminals with interactive control.

TABLE OF CONTENTS

INTRODUCTION

The theory of plate tectonics, developed primarily during 1963-1975, gave us a completely new, dynamic view of the Earth and explained essentially all of the new observations from the ocean floors. It does less well in continents, because continental plates are softer and less rigid, and because their buoyancy keeps them on the surface of the Earth forever, where they accumulate complexity. As we strive to go beyond plate tectonics and understand the deformation of continents, we need the computer as an experimental tool.

This paper has two parts. First, it gives a qualitative description of the mathematical tools and strategies that have been developed for modeling continental deformation, including several new contributions. Second, it shows the first application of these new tools, to model the Cenozoic history of North America, and test several long-standing hypotheses. Although our computed predictions do not and cannot match the resolution and wealth of detail that field geologists work with, still this simulation appears to be a success in a broad sense. I present a dynamically consistent model of how plate motions around and beneath North America caused it to be first shortened, then uplifted, then extended, and even locally rotated. From such studies, it should be possible to determine the flow-law, or rheology, of the continental plates.

COMPUTER MODELS FOR GEOLOGY

Structural geology and its recent offspring, tectonophysics, have been slow to take their places among the rigorous, quantitative "hard" sciences. For all the efforts of thousands of field geologists, we still do not have detailed knowledge of enough deformational events (*orogenies*) to study them by purely empirical means. There were basically two problems: the lack of a central paradigm, and the inability to conduct experiments.

The paradigm has now been provided by the theories of plate tectonics and mantle convection. More recently, computer modeling of deformation has added the ability to actually experiment with plate-margin processes, such as *rifting* (the separation of two plates, with the upwelling of fresh crust between them) and *subduction* (the underthrusting of one plate beneath another). While it has always been possible to model the simplest deformation geometries with a scale model of an elastic material, or a viscous material, or a frictional material, only the computer can combine these flow-laws (*rheologies*) in a realistic way, and add nonlinearity, temperature-dependence, and heat-conduction effects. At last we are able to approach continental-size problems, and test whether the boundary conditions from plate tectonics and the rheologies obtained in the rock-mechanics laboratories can be combined to "predict" ("postdict"?) actual mapped structures. If not, then some fundamental aspect of the physics has been overlooked, and we have a chance to improve our understanding.

Deformation modeling can be imagined at four scales; the benefit/cost ratio varies widely, and generally improves with the size of the problem.

* "Grain-scale models" of stress and strain inhomogeneities are in their infancy, and have usually been quite idealized (*e.g.*, elastic or isotropic-plastic, regularly packed grains). There are formidable difficulties in representing the fine structure of actual grain boundaries, subgrain walls, kink bands, *etc.*- especially since much of their basic physics is unknown. Furthermore, the high cost of realistic models will always exceed the cost of an actual experiment, which has the further advantage of automatically obeying the proper physical laws.

* "Outcrop-scale" models are concerned with the effects of contrasts in strength between different rocks in creating faults, folds, boudinage, *etc.* This is historically the first of the modeling disciplines to develop (*e.g.*, Stephannson and Berner [36]; Parrish *et al.* [34]). It is usually reasonable to assume isothermal and plane-strain conditions, so the cost of simulations is moderate and supercomputers are not essential. The virtue of this approach is that potentially the rheologies of the rocks could be cross-calibrated, if pressure, temperature, and strain-rate could be independently determined from the chemistry of the rocks. The weakness of the method is that the boundary conditions and initial conditions can only be guessed in most problems.

* "Quadrangle-scale models" would attempt to predict actual geologic maps, in order to test tectonic hypotheses or calibrate rheologies. To my knowledge, they have never been attempted in three dimensions. The outstanding difficulty is not cost, but the ignorance of bottom boundary conditions, which will usually dominate the results.

* "Continental-scale modeling" is clearly the growth area in computational tectonophysics. This is due to the happy conjunction of: (1) a weak, quasi-fluid bottom boundary provided by the hot interior of the mantle (the *asthenosphere*, or "shell of no strength"); (2) velocity boundary conditions on the edges provided by plate tectonic theory; (3) direct constraints on present surface velocities from geodesy, and on strain-rates from seismicity; and (4) constraints on net strain from published maps of crustal thickness, geologic structures, and surface heat-flow.

Such modeling began with two-dimensional plane-strain cases, the model plane being a vertical cross-section (Zagros mountains: Bird [2], Rhine graben: Neugebauer [33], Himalaya: Wang *et al.* [41, 42]). Thermal structures were simply assumed, and velocities were computed from realistic nonlinear rheologies for qualitative hypothesis-testing. Typically, the lack of data on deep underground structures limits our ability to test the success of these models.

The restriction to two dimensions was overcome using the "thin-plate" modeling technique, which is said to be "2.5-dimensional." That is, finite element grids cover only latitude and longitude, yet the strength of the plate is evaluated using numerical integrals in depth as well as area (California: Bird and Piper [12], Bird and Baumgardner [11]; Tibet: Vilotte *et al.* [38, 39, 40], England and Houseman [21], England and Searle [23], Sonder *et al.* [35], Houseman and England [26]; England and Houseman [22]; Cohen and Morgan [14]).

Taking advantage of the versatility of finite element techniques, I have developed ways to incorporate many realistic complexities: realistic frictional rheologies for the upper crust, faults, soft "detachment" horizons in the lower crust, lateral diffusion of crustal thickness, complex boundary conditions, and internal heat-conduction. The work presented in this paper represents the highest level of realism ever attained in such modeling. Of course, the cost is also high- on the order of 5 supercomputer minutes per million years of simulated time, when the problem is as large as North America. Predictions of such models can include the map patterns and histories of velocity, rotation, strain-rate, stress, crust and lithosphere thickness, surface elevation, heat-flow, and seismic-velocity structure- so the opportunities for testing and validating models with published data are numerous.

COMPUTATIONAL METHODS

Mathematical Methods

The problem of simulating continental deformation is an initial-value problem in the Stokes creeping-flow equation, linked with the heat-diffusion equation, and subject to a complex mixture of velocity and stress boundary conditions. The complete derivation of the model equations is given in Bird [7]. Such calculations are difficult because the strength of rocks is exponentially dependent on temperature (at least above some transition or "softening" temperature), and the temperature gradients in the lithosphere are large, and they depend on the deformation. The typical duration of the model (*e.g.*, 85 million years) is such that neither an adiabatic nor a steady-state approximation of temperatures is adequate. Thus, the calculation proceeds through timesteps (of order 1 million years), each of which is artificially partitioned into an adiabatic translation and a static period of heat diffusion.

The model domain includes the crust and mantle lithosphere of a continent, which is very much wider (*e.g.*, 5000 km) than it is thick (100 km). Therefore, it is an adequate approximation to solve the Stokes equation in vertically-integrated form, effectively condensing the strength of the lithosphere into a single plane. The horizontal components of velocity are then computed by the "thin-plate" finite element method. That is, two-dimensional finite-element grids are used to represent the strong crust and mantle-lithosphere layers, but their assigned properties reflect the results of three-dimensional volume integrals throughout the layers (Figure 1). This method reduces the finite-element grid from 3 dimensions to 2, with an indispensable reduction in cost. Vertical force equilibrium is represented by the *isostatic approximation*, which is that each column floats independently on a fluid support at an elevation determined by its density structure. Time integrations are performed by the predictor/corrector scheme, requiring the iterative solution of nodal velocities to be performed twice in each timestep. The finite element grid deforms over time to follow the path of the more rigid material at the top of each layer. Occasionally, manual gridding of highly deformed regions in the mantle layer is required.

One major innovation in this project is the use of two stacked grids to represent the crust and the mantle lithosphere layers of North America respectively (Figure 1); this allows their velocities to differ, which is an essential feature of the proposed geologic history of North America. The vertical integration of strengths is performed numerically at each of 7 Gauss integration points in each finite element. A simultaneous vertical integration of compliance (inverse of effective viscosity) provides the coefficients necessary to compute the shear stresses between the layers when their horizontal velocities differ.

The rate of thickening of each layer is determined by the incompressibility condition, which is exact for all anelastic strains. Like displacement, layer thickness is assumed to be laterally continuous, and is parameterized by quadratic finite-element basis functions. One effect causing thickness changes is (i) divergence, in the horizontal plane, of the horizontal velocity of the grid which represents the strong upper part of each layer. This will be referred to as "pure shear" since it is irrotational in any vertical cross-section. A second effect is (ii) divergence, in the horizontal plane, of the flux of ductile material that is involved in "simple shear" to accommodate different horizontal velocities of layers. This flux depends on the difference between the horizontal velocities of the grids, and on the vertical temperature gradient, which determines the thickness of the simple-shear boundary layer. The third effect is (iii) independent flow of ductile material in response to lateral pressure gradients associated with topography ("gravity spreading"). In the crust, this effect tends to smooth the thickness through a nonlinear "diffusion" of crustal thickness (Bird [9]). Effects of erosion and the deposition of sediments on crustal thickness are neglected.

The preliminary model presented in my previous report (Bird [6]) had all three of these effects compressed into a finite element computation of layer thickening, which shared the same large timestep (e.g., 1 million years) as the velocity calculations, and was also integrated by the predictor/corrector method. The equations for this method were presented in Bird [7]. However, two important improvements have been made since that time.

Effect (ii), the layer-thickening caused by simple-shear advection, was not handled well by finite elements. As other sources of noise were gradually eliminated, I came to see that this term was sometimes causing a bounded instability. Similar problems with advection terms in other finite element codes have been controlled with "upwind" schemes, but these do not have a strong theoretical basis. Instead, I chose to compute the advection by collocation (i.e., at specific points only), and accomplished this by using Runge-Kutta integration of the velocity fields to find the upstream point that would be advected beneath them during the duration of the timestep. Then, a smooth function (spanned by the finite-element nodal functions) was fit to the values computed at these points.

Effect (iii), the lateral diffusion of crustal thickness and topography, is sometimes extremely rapid. Because of its nonlinearity, no explicit integration method has been found. Therefore, it is necessary to use explicit or predictor/corrector integration and to restrict the timestep to avoid instability. However, the timesteps required (circa 100 years, in some cases) would be prohibitively short if propagated throughout the calculation. Therefore, I reprogrammed this effect as a diffusion equation on a distorted finite difference grid (defined by the finite element nodes), and solved it using very small "inner" timesteps nested within the "outer" timesteps of the horizontal-velocity solutions. The finite difference computation is explicit, for speed, but it is periodically interrupted to update the diffusion coefficients, so as to reflect the nonlinearity. Frankly, this effect is not computed with very good precision- however, this is the first time it has been simulated at all!

In the computation of temperatures, lateral heat conduction is insignificant, and is neglected. At each of the 7 Gauss integration points in each of the elements, the *geotherm* (temperature as a function of depth) is represented as the sum of steady-state quadratic functions and a set of 5 decaying eigenfunctions of the homogeneous one-dimensional diffusion equation. Wherever simple shear between layers would tend to cause a temperature discontinuity at the base of a layer, this is corrected by adding an appropriate cubic term to its geotherm. Shear-strain heating computed by the momentum-conservation part of the code was used as a source term in this thermal energy-conservation section. These are both techniques first introduced in this project; previous models by other authors have all neglected shear-strain heating, and have assumed linear geotherms, partly because they lacked the mechanical degrees of freedom necessary for detachments on horizontal planes, which destroy this linearity by a complex advection of heat.

Convergence tests documented in Bird [7] suggest that the results presented in this paper have a relative precision (RMS error/RMS signal) of about 15% for the variables of crust and mantle displacement, and mantle thickness. However, the changes in crustal thickness have only about 50% RMS relative precision, and should be considered as suggestive rather than definitive. Greater precision is not presently attainable, as each run already consumes about 6-8 hours on an IBM 3090/VF (using one processor). The main reason for this expense is that the nonlinearity of the rheology requires the velocity solution to be iterated about 15 times per timestep, the historical nature of the problem requires about 100 timesteps per model, and our ignorance of some parameters requires a number of models

Implementation on an IBM System

This modeling program was developed in VS-FORTRAN, at UCLA, and the calculations described below were executed on UCLA's most recent mainframe, an IBM 3090 with Vector Facility. Because of the strong nonlinearity of the problem, and the need for iterative solutions in each timestep, CPU limits are more important in practice than memory limits. With 609 nodes and 280 elements per layer, this code requires a relatively modest 5 megabytes of memory. (However, it is also true that the installation of the MVS system at UCLA, early in the history of this project, made my progress much more rapid; the reason was that previously I had only been able to obtain this amount of memory during the night.)

The three most time-consuming parts of the calculation are (1) the repeated vertical integrations of strength and compliance beneath each of the Gauss integration points of each of the elements; (2) the repeated solutions of linear systems resulting from the finite element approximation, and (3) the finite difference solutions of the equations for the lateral diffusion of crustal thickness and topography. The first was made vectorizable by subdividing the vertical integrals into an equal number of steps for each Gauss point, and advancing these integrals downward in an outer loop, with an inner loop over all the Gauss points. This is a good example of how vectorization is often achieved at the cost of extra storage, because I only accomplished this by creating new memory arrays for intermediate results. The solution of the linear equations was handled by prevectorized banded-matrix routines from the Engineering and Scientific Subroutine Library, which were very satisfactory. The finite difference code was written so that it involved only vector dot products in the inner loops; hence this code achieved essentially the full speed possible on a single Vector Facility, permitting approximately 1,000 "inner" finite difference timesteps to be performed in CPU time of about 30 seconds, and nested within each "outer" finite element step. The most time-consuming non-vectorizable routines are those that evaluate the rock rheology and assemble the coefficients for the linear system; the problems with these are multiply-branching logic and indirect-addressing, respectively. In summary, the code achieves about 50% of its CPU time in vector mode, and execution times are 6-8 hours per model with vectorization. (The time in scalar mode would be approximately 45 hours, which is clearly impractical.)

The main program runs as a batch job. However, interactive accessory programs were also written in VS-FORTRAN to assist in the preparation of plate reconstructions, editing of initial-condition files, and preparation of color contour maps of the output through time. These programs also require the 3090's speed, but provide graphics output, through the interface of Graphical Data Display Manager software, on IBM 3179 terminals. The b/w figures presented here were created by similar code driving a Versatec electrostatic plotter.

GEOLOGIC HISTORY OF NORTH AMERICA

The Problem of the Laramide Orogeny

The formation of the Rocky Mountains, in an event known as the "Laramide orogeny," has been studied by geologists for a century. However, for most of that time, they had to work without any clear concept of the overall driving force or mechanism. Only since 1978 have we understood how plate-tectonic events occurring at the west coast could so profoundly affect the interior. With this understanding has come an appreciation that the simultaneous uplift of the entire Rocky Mountain region and the Great Plains deserves to be considered part of the Laramide orogeny.

It has long been known that deformation began in the Late Cretaceous epoch, peaked in the Paleocene, and waned in the Eocene. All mountain ranges (and many smaller structures which have been explored in the search for oil) show evidence of minor horizontal shortening of the crust in the east-west or northeast-southwest direction. This event clearly deformed, and locally uplifted, the layer of the crust that was last deformed and metamorphosed in Precambrian time (the *basement*) as well as the thin veneer of younger Paleozoic and Mesozoic sedimentary rocks. Today, these basement uplifts still correspond to topographic ranges, such as the Beartooth Mountains of Montana, the Wind River and Big Horn ranges of Wyoming, the Front Range of Colorado, and the Sangre de Christo mountains of New Mexico (Figure 2). Although there has been much controversy over the exact mechanism of basement uplifts, nearly all workers would probably agree that the total shortening in Wyoming was roughly 5% (Couples and Stearns [15]) to 10% (Gries [24]).

Another major problem is that this shortening is not enough to explain the thickening of the crust (from about 39 km to over 55 km) that also occurred during the Laramide orogeny (Bird [5]), and that currently helps to support the high regional elevation. Thickening of the crust by igneous intrusions was three orders of magnitude too small to explain this, even under generous assumptions about the shape of intrusive bodies (*ibid*). Therefore, some mechanism involving larger strains in the ductile lower crust must be inferred. One additional complication is that most of the Laramide basement uplifts were sediment-covered during their formation, only emerging to become topographic features after the end of Laramide time (Trimble [37]).

The concept that the Rockies might have been formed by "subcrustal convection currents" goes back at least to Longwell [30], who applied the concepts of Arthur Holmes and David Griggs to this region. These early writers conceived of the crust (the surficial layer, 5-75 km thick, which is distinguished by its more silicic composition) as rigid/plastic, and thought of the underlying mantle as a uniformly fluid layer of no long-term strength; an *asthenosphere*. Now, under the modern theory of plate tectonics, we postulate that the top of the mantle contains a cold, rigid thermal boundary layer (the *mantle lithosphere*) that overlies the asthenosphere. We also have the advantage of the historical record of paleomagnetism, which demonstrate conclusively that vast areas of oceanic crust and attached lithosphere were *subducted* (underthrust) beneath the west coast of North America during this time (Atwater [1]; Engebretson *et al.* [20]). A link between subduction and the Laramide orogeny was suggested by Dickinson and Snyder [19], who proposed that the subduction was horizontal, with the oceanic lithosphere sliding along the base of North America as far inland as the Black Hills of South Dakota (Figure 3). They suggested that the resulting shear stresses caused the shortening strains seen at the surface. Horizontal subduction has also been invoked to explain the sudden subsidence of the region in the Late Cretaceous (Cross and Pilger [17]). Finally, I have previously suggested (Bird [5]) that horizontal subduction transferred crustal material into the Rockies region from the southwest, increasing the crustal thickness by about 65%.

In this paper I present a numerical test of the hypothesis of flat subduction, by a quantitative prediction of its effects. The boundary conditions of the simulation are obtained from plate tectonic theory and are reasonably certain.

Boundary Conditions from Plate Tectonic Theory

The northern, eastern, and southern margins of the finite-element grid (Figure 4) were fixed. Boundaries in Mexico and Canada were placed where Laramide strain becomes secondary to the effects of other Tertiary orogenies that are not modeled- those in the Caribbean and in Alaska. The eastern and Gulf-coast boundaries are natural; the strength of oceanic lithosphere is so much greater than that of the continental lithosphere that strain will be negligible in the former, and therefore displacements must be small at the continental margins. The western edge of the continent is the upper plate of a subduction zone (Figure 3), so this edge is tapered to a line, and does not require a boundary condition, as it has no surface area.

At each timestep, the bottom boundary can be divided into two areas which receive different treatment: the area overlying normal hot asthenosphere, and the area overlying flat-subducting oceanic plate. This oceanic plate was probably part of the large plate known as the Farallon plate (Figure 5), of which only small fragments remain today, offshore of the Pacific Northwest and southern Mexico. (It may alternatively have been the Kula plate; this possibility is discussed below.) The boundary between these areas moved inland and then westward again (Figure 6) during the interval modeled, and its progress may be tracked by the changing patterns of volcanism in the western United States (Dickinson and Snyder [19]).

Where mantle lithosphere overlies asthenosphere, its basal temperature was fixed at 1175 C. (In nature, a similar boundary condition would be enforced by mantle convection.) However, wherever unprotected cold crust overlies this hot asthenosphere, the crust will be heated while a (relatively) cold thermal boundary layer will begin to form at the top of the mantle (a new mantle lithosphere). Since the preliminary model of Bird [6], I have added a computation of the formation of such new lithosphere for use in the thermal model of the crust, and for use in calculating elevations. (However, I have not provided new finite elements to represent the strength of the new layer, which is negligible during the time interval modeled.) Mechanically, the North American plate is supported on a perfectly fluid asthenosphere (with density 3150 kg/m^3) in which there are no shear stresses.

Where the North American plate overlies flat-subducting oceanic plate (Figure 6), it is subject to both horizontal and vertical tractions. To determine the anomaly in the vertical traction, I found the excess mass of the oceanic slab (with respect to the asthenosphere it displaces). To do this, I first reconstructed the subducted parts of the Farallon plate, using Eulerian finite rotations on the Earth's spherical surface, which I obtained from Engebretson *et al.* [20]. I then applied the standard boundary-layer cooling model of oceanic lithosphere by assuming that its vertically-integrated excess weight with respect to asthenosphere is [6600 Pa] $\times \mathbf{t}^{1/2}$, where $\mathbf{t}$ is its age (cooling time), in years. The normal fluid support pressure on the bottom of North America was reduced by this amount, so that after isostatic adjustment the surface of the continent was depressed by about 2 to 3 km over the flat-slab region (Cross and Pilger [17]; Bird [5]). The horizontal velocities of the slab were obtained from rotation poles of Engebretson *et al.* [20], and are used as velocity boundary conditions on the area contacted. Note that velocity is imposed on the weak base of the bottom layer, and the velocity of its strong upper levels and its finite-element grid will usually be less, depending on rheology and temperature. Also, the shear stress necessary to impose this velocity boundary condition is monitored, and if it exceeds 27.5 MPa then a shear stress boundary condition is substituted (to simulate formation of a ductile fault). The appropriate value of this stress limit is one of the more uncertain of the model parameters, although I had some guidance from values inferred in other subduction zones (Bird [3]).

Where this slab makes contact with the base of North America, a temperature boundary condition was also imposed. The imposed temperature is initially 10 C at the coast, and increases inland according to a cube-root-of-distance law, reaching 380 C at 1000 km from the coast. This function is a good approximation of the results obtained in a two-dimensional finite-difference model of heat advection and diffusion (including the oceanic plate in the domain) that was conducted separately in a representative cross section. (This is an additional improvement over the model reported in Bird [6].) Note that the imposed boundary temperature is lower than the initial temperature at the base of either crust or mantle, so that the thermal effect of the slab is to cool and strengthen the parts of the continent that it touches. Thus, the orogeny is definitely produced by the mechanical (traction) effects of the flat slab, and is actually hindered by its thermal effects.

Rheology of North America

In these calculations the total strains of interest range from 0.05 up to 100, so the contribution of elastic strain is negligible. Deformation is governed by one of three laws, each based on laboratory experiments, which place upper limits on the shear stress magnitude $|\mathbf{p}_s|$. Each law is written for an isotropic material, partly for simplicity and partly out of ignorance. At low temperature, the important limit is set by frictional sliding on any and all planes:

$$|\mathbf{p}_s| < \mathbf{f}\,(|\mathbf{p}_n| - \mathbf{P}_{water})$$

where $\mathbf{f}$ is the coefficient of friction, $|\mathbf{p}_n|$ is the magnitude of the normal stress on the same plane, and $\mathbf{P}_{water}$ is the pressure of water in pores (assumed hydrostatic). At higher temperatures, the relevant limit is set by thermally-activated, power-law dislocation creep:

$$|\mathbf{p}_s| < 2\,\mathbf{A}\,\{2(-\mathbf{e}_1\mathbf{e}_2 - \mathbf{e}_2\mathbf{e}_3 - \mathbf{e}_3\mathbf{e}_1)^{1/2}\}^{(1-\mathbf{n})/\mathbf{n}}\ \ \mathbf{e}_s\ \exp\{(\mathbf{B} + \mathbf{C}\,\mathbf{P})/\,\mathbf{T}\}$$

where $\mathbf{e}_i$ are the principal strain rates, $\mathbf{e}_s$ is the shear strain rate (on the same plane as $\mathbf{p}_s$), $\mathbf{P}$ is total pressure, $\mathbf{T}$ is absolute temperature, and $\mathbf{A}$, $\mathbf{B}$, $\mathbf{C}$, and $\mathbf{n}$ are empirical constants ($\mathbf{n}$ is approximately 3).

The third limit is a plasticity condition which is independent of $\mathbf{P}$, $\mathbf{T}$ and $\mathbf{e}$: $|\mathbf{p}_s| < \mathbf{p}_p$.

In applying all of these laws, the vertical stress $\mathbf{p}_{zz}$ is assumed to be *lithostatic* (equal to the weight of the overburden per unit area). To avoid numerical difficulties, an upper limit is also placed on the effective viscosity at all points.

It should be noted that two of these parameters ($\mathbf{A}$ and $\mathbf{B}$ of the crust) were adjusted to values that gave the proper magnitude of Laramide surface strain. I found that it was not necessary, or possible, to change the friction $\mathbf{f}$ from its starting value of 0.85.

Initial Conditions, in the Cretaceous Period

The model begins 85 million years ago, in the Late Cretaceous epoch. At that time, the future Rocky Mountain region and Great Plains were close to sealevel, and had been since the late Cambrian epoch (Mallory [31]). (A belt from eastern Utah to the Texas panhandle was deformed in the late Paleozoic Ancestral Rockies orogeny, but this topography had been completely eroded by Laramide time.) Therefore, I assume that heat diffusion had established a uniform steady-state geotherm with a typical platform heatflow of 54 mW/m^2, and that the combination of isostasy, erosion, and deposition had leveled the crust to a uniform thickness of 39 km. The initial thickness of 70 km chosen for the mantle lithosphere is somewhat arbitrary, since the lithosphere/asthenosphere boundary is gradational. Because the strength of this layer is concentrated at the top, the lower limit of integration makes little difference.

Much has been written about the probable influence of earlier structures (such as the Ancestral Rockies) on Laramide deformation. Unfortunately, such structures cannot be included in the model. There is a problem of resolution, and a more significant problem that the structures are only known where Laramide uplifts caused erosion to strip off the sedimentary cover and expose them. To include these, while omitting all buried structures, would unacceptably bias the results. I feel that we should first determine how much geologic history can be understood through homogeneous continuum models, before adding such complications.

Further west, within about 600 km of the coast, there was a mountain belt comparable to the present Andes (Figure 7). This had developed during the previous 130 million years above a subduction zone of typical geometry, and its eastward spreading under the force of gravity was responsible for the Cretaceous "Sevier orogeny" which formed the Overthrust Belt just prior to the Laramide events (Burchfiel and Davis [13]). My model of the structure of this coastal cordillera is based on an analogy; I adopted the structure of the Andes at 23°S, as determined by Grow and Bowin [25].

A Successful Simulation

(The following account is a qualitative description of the model I denote as 89-28, which subjectively appears to be the best to date. A description of the subtle differences between models will follow.)

In the first 5 million year of the calculation (the Campanian age of the Late Cretaceous epoch), there is normal subduction at a steep angle, and the coastal cordillera remains stable; strain rates are below 10^{-16}/s in the interior of the continent. As the flat-subducting slab of oceanic lithosphere begins to slide along the base of North America (at 80 million years ago), it initially contacts the base of the mantle lithosphere, at about 100 km depth. The cold slab chills and strengthens this mantle lithosphere, forming a "mantle plate" that subsequently moves northeast without internal deformation or thickening; deformation occurs in the surrounding mantle lithosphere that has not been touched or chilled. Although the shear stress applied to this strong edge is limited to 27.5 MPa, the cumulative force transmitted over a broad area sets the entire mantle lithosphere of North America in motion to the northeast (with respect to the crust), at up to 8 cm/year (Figure 8). The mantle lithosphere moves without greatly displacing the upper crust, from which it is detached by a weak shear zone in the lower crust. The mantle lithosphere shortens horizontally and thickens vertically by pure-shear strain, and is finally left beneath the northern Great Plains.

After the mantle lithosphere is removed, the oceanic plate drags directly on the base of the crust. The crust is also chilled and strengthened, and thus in most places it only moves at a very small fraction of the slab velocity. An assumed simple-shear zone in the subducted sediments on the top of the slab accommodates the relative velocity across most of the interior, and prevents the shear traction from rising above the value observed in other systems.

However, the great thickness of the crust in the higher parts of the coastal cordillera (60-75 km) prevents this chilling from affecting all of the ductile, creeping part of the crust. In this region, the geotherm retains a local maximum temperature at 30-40 km depths, where there is consequently a shear zone and a detachment horizon. The consequence is that the deeper parts of the cordilleran crust are sheared away and transported to the northeast. Since the scale thickness of this shear zone is only 5 to 10 km and the relative displacement is of order 1000 km, shear strains of order 100 accumulate in the middle crust (which becomes the lower crust after the deeper parts are removed). The crust is thinned in the cordilleran region, causing the coastal mountains to disappear. Simultaneously it is thickened in the Rocky Mountain region, causing an buoyant (isostatic) uplift (Figure 9). This crustal thickening in the Rockies gradually reversed the initial subsidence that had been caused by the weight of the slab of oceanic crust and lithosphere.

In the strong upper crust, horizontal compressive stress is generated by these basal tractions, as suggested by Dickinson and Snyder [19]. This stress is largest at the northeastern margin of the region of flat subduction, as required by the stress equilibrium equation. In addition, this relatively depressed region has less vertical topographic stress, which always tends to resist horizontal shortening. This is why surface shortening strains concentrate in an arc from Montana to New Mexico in all models, regardless of the rheological parameters. This finite element grid does not have the spatial resolution to predict individual structures like the Wind River or Big Horn ranges, but it does consistently predict a curved belt of crustal compression with the correct location, timing, and orientation (Figure 10). (In this particular model, the average net strain in Wyoming has been adjusted to 11% shortening by experimenting with the crustal rheology.) The maximum strain rates at the surface occur when the flat slab area reaches its maximum width, about 60 million years ago, in the early Paleocene epoch.

Later, the region of flat subduction contracted (Figure 6), and the inland volcanic arc which marks its eastern limit returned westward toward the coast. Published paleomagnetic data from the present Pacific basin rule out any reversal of oceanic-plate motions, so we must conclude that the hingeline surrounding the flat-slab area moved west while the slab continued to move east. (There is no particular dynamical difficulty in this, as hingelines are always already moving in the reference frame of their slabs.) Consistent with the continuum approach, I assume that the oceanic slab peeled away and sank as a continuous sheet, without leaving any fragments attached to North America.

This exposed the base of the crust to upwelling hot asthenosphere over a vast region west of the Rockies. Heating from below decreased the strength of the crust progressively over about 10 million years (Bird [4]), while isostatic rebound increased its elevation, and therefore the tendency for gravitational spreading. Thus, crustal extension becomes likely several million years after the removal of the flat slab, but only in the regions from which the mantle lithosphere has been removed. This explains why the later Basin-and-Range extension event (*taphrogeny*) was confined to the part of North America west of the Rocky Mountains.

There has been a controversy for 25 years about the dynamics, or driving stresses, of this extensional event. One school of thought begins with the observation that the crust was heated and elevated in the Tertiary time (although until now the mechanism for this was unknown). It concludes that this was sufficient cause, and that the spreading was driven by gravity, as in a continental icecap. I was initially of this opinion, and in fact presented such a model in Bird [6].

However, the improvements that were made to this modeling code in 1989 (principally in the thermal model) required that the crustal rheology should be made stiffer, in order to still obtain the correct, modest shortening strains in the Laramide orogeny. After making these adjustments, I no longer found the same gravity-spreading behavior. Instead, the continuing subduction along the west coast provided just enough horizontal compression to offset the gravitational forces, and the crust became static from the end of the Laramide shortening until about 30 million years ago, in the middle of the Oligocene epoch.

At that time, a second extension mechanism, first proposed by Ingersoll [28], became active. This was the time when the divergent, or spreading, boundary between the Pacific and the Farallon plates first met North America, and began to subduct. This caused a topologic reconnection of plate boundaries, after which North America was directly connected to the Pacific plate in the region of southern California. The Pacific plate motion was generally to the northwest, and so a *transform fault* (one with relative motion parallel to its length) was formed, which later became the San Andreas Fault system. The critical point, first noted by Ingersoll [28], is that the Pacific motion was probably *not* exactly parallel to the Oligocene continental margin. Therefore, North America was required to stretch.

This effect was included in the model by adding a group of linear fault-simulating elements to the western edge of the crustal grid at the appropriate latitudes and times. The boundary condition on the southwest side of these elements was the velocity of the Pacific plate. Their sliding stress was set to a relatively low value of 27.5 MPa, consistent with present-day studies of the San Andreas Fault. And, naturally, we observe the behavior predicted by Ingersoll. Extension begins (Figure 10) in the southern California region, and spreads by about 20 million years (early Miocene time) into Arizona, Utah, and Nevada. Lesser amounts of extensional strain are predicted in southern Idaho from about 15 million years ago, and in New Mexico from about 10 million years ago. The prediction for the present day is that extension should be active in central Nevada, southwest Arizona, and in all of western Mexico.

One last feature of the model is local and poorly resolved, but very interesting. The extensional traction that the Pacific plate exerts on the coast in the southern California region is locally intense, but has well-defined latitude limits determined by plate geometry. At the northern end of the region of tractions (which travels with the Mendocino Fracture Zone on the Pacific plate) there is a traction couple, with a westward pull to the South, and an eastward push (from continuing subduction) to the North. Because the crust is locally weakened by basal heating (where the East Pacific Rise passes beneath North America) this traction couple causes large local rotations about a vertical axis, in a clockwise sense. Some of the predicted rotations are as large as 60 degrees (Figure 11).

Predictions vs. Data- A Preliminary Comparison

The literature on the Cenozoic geologic history of North America is vast. Concentrating only on the central region, I have amassed a bibliography of 1,000 references containing potentially useful data on past stresses, strains, or topography, as well as present-day data such as seismicity, heat-flow, and seismic structure. When this is collated and digitized, an objective, quantitative ranking of the models will be possible; this will be presented in a future monograph. Here, space limitations allow for only a cursory mention of the best and worst features.

Surface Strain-Rates. According to Dickinson *et al.* (1988), the duration of the Laramide orogeny is bracketed between a beginning at 70 Ma and an end which swept South during 57-35 Ma. In our model, shortening begins promptly at 70 Ma in British Columbia-Montana-Wyoming-Colorado-New Mexico (Figure 10). It continues at very low rates (e.g., 2×10^{-16}/s), with a diminution in intensity at 60-50 Ma, until 37 Ma. There is a striking resemblance to the well-known belt of Laramide basement uplifts in these states (Figure 2), including coincidence of their long axes (which would be parallel to thrust fault trends). The model does not reproduce the North-to-South progression of the cutoff.

Following Laramide compression came extension, which also progressed North-to-South, beginning in British Columbia about 52 Ma, and reaching southeastern California about 15 Ma. My earlier model (Bird [6]) predicted the early part of the extension well; it is frustrating that this feature has been lost as improvements in realism have required a stronger crustal rheology. The model still shows, however, a wave of increased heat-flow in the correct places and times. Possibly, the real upper crust was weakened by local granitic intrusions above each of the sites of extension ("metamorphic core complexes") as some geologists have already proposed. In the model, extension gets underway at the time of the intersection of the East Pacific Rise with the continental margin, at 35 Ma. It spreads by about 20 million years into Arizona, Utah, and Nevada. Lesser amounts of extensional strain are predicted in southern Idaho from about 15 million years ago, and in New Mexico from about 10 million years ago (Figure 10). This last feature is realistic, as the opening of the Rio Grande Rift began by 15 Ma, but did not really accelerate until 10 Ma (Ingersoll *et al.* [29]). A very strong concentration of predicted extension in coastal Mexico from 10-5 Ma could be interpreted as the model's attempt to reproduce the rifting of Baja California, which occurred at that time. The prediction for the present day is that extension should be active in central Nevada, southwest Arizona, and in all of western Mexico. Overall, the map pattern of extended regions is quite realistic.

In the last timesteps (5-0 Ma) the model predicts rapid strike-slip faulting in California. This is analogous to the formation of the San Andreas fault system, although of course a more sophisticated program will be needed to model the shuffling of small crustal blocks that actually occurred.

Topography. Unfortunately, the only feature of past topography that is well known is the position of shorelines. The model succeeds in matching several important features. First, it predicts the appearance of a marine basin in southern Wyoming, western Colorado, and eastern Utah at 75 Ma (Ma = million years ago). This is due to the excess mass of the subducted Farallon plate dragging down the overlying part of North America. Such a basin actually did form during the period 84-66 Ma (Cross and Pilger [17]; Cross [16]) as shown by thick deposits of black shale. In the model, this basin shrinks as a moving wave of high ground compresses it from the West; a similar migration of the real shoreline is documented in Mallory [31]. The model basin loses its marine connection (becomes a lake) and progressively shallows until it disappears at 40 Ma. Interestingly, the predicted topography in Eocene time (58-37 Ma) is fragmented into 5 basins, much as the actual Rocky Mountain foreland was. The model topography loses all of its basins and becomes convex about 35 Ma, about the time when basin sedimentation actually ceased in the Rockies.

The second, late Cenozoic uplift of the Rocky Mountain foreland that was inferred by Trimble [37] is not seen in the model. However, if we assume that the overthickened part of the mantle lithosphere in the region was later removed by convection Houseman *et al.* [27] or delamination (Bird and Baumgardner [10]), then the model could be consistent with a second late uplift of about 1 km amplitude. Such "convective" behavior is not predictable by our techniques.

The predicted topography for the present day is quite accurate, except for excessively high ground in eastern Montana and British Columbia (Figure 7).

Net Cenozoic strain (Figure 2). The integrated compressive strain in the Rocky Mountain foreland has been set to a reasonable 11% by adjustment of the crustal rheology. The predicted trends of thrust faults swing from N-S in New Mexico to NW-SE in Montana, in excellent agreement with the actual uplifted ranges. Generally, the belt of shortening is about 200 km too far East; this may reflect errors in either the assumed hingelines of the flat subduction, or in the initial coastline of North America.

The province of net extensional strain is approximately the right shape, but should be somewhat larger- it should extend into western Utah and southwest Idaho. Generally, the model predicts too much of a concentration of shortening along the coastline. Such behavior is a reasonable response to the higher heat-flow there, and in this case it is the behavior of the real Earth that is not well understood. Perhaps some weakening mechanism (*i.e.*, an influx of subducted water?) which is not included in the model was responsible for making the topographic stresses relatively more important, and thus distributing the strain more widely.

Clockwise Rotations. The model prediction of large clockwise rotations in California was discussed above. Similar rotations (and larger ones, up to 120°) have been documented by Luyendyk et al. (1985) in the Transverse Ranges province of California (Figure 11). While this is intriguing, there is also a problem: the model rotations extend too far North, to the latitude of San Francisco. They would extend even further North, to the Mendocino Fracture zone, if transport of the rotated regions by the San Andreas Fault were included. Thus, the model is clearly wrong in detail, but it may be suggesting a valid concept. This needs to be explored in detailed models of the local region, with far better resolution.

Present Mantle Lithosphere. Of course, the mantle lithosphere can only be observed by seismic methods, and only in the present. The model predicts that the old lithosphere has been removed west of a line from central Montana through western Wyoming, Colorado, and New Mexico (Figure 8). It may be worth designing seismic experiments specifically to find this boundary. In New Mexico, Davis *et al.* [18] have shown a pronounced asymmetry, with much thicker lithosphere to the East. I interpret this as showing that the edge of the old lithosphere was displaced to the longitude of the rift (i.e., *further* than in the model) and that the thinner lithosphere to the west represents a new layer formed by cooling in the last 30 Ma.

Crustal Thickness. The predicted present thickness of the crust (Figure 9) agrees well with a compilation of seismic refraction results presented by Mooney and Braile [32]. Both show a ridge of thicker crust extending down the center of the United States from Montana to New Mexico. The prediction is only seriously incorrect in British Columbia, where actual thicknesses are normal (35-40 km), but high values are predicted.

Experiments with the Model

Although attention naturally focuses on the best model obtained, *any* model experiment conducted with such an investment of computer time should add something to our knowledge. In the set of 18 simulations that I was able to perform with this program, about half were used to test for sensitivity to initial and boundary conditions, while the other half were devoted to testing variations in the rheology of North America. Complete results of the set will be presented in a future monograph.

Among the boundary-condition tests, most resulted in very small changes, and were therefore inconclusive. The most interesting variation tested was a major modification to the reconstruction of the oceanic plates. As Engebretson *et al.* [20] discovered, it is possible to reconstruct the plates so that it is the Kula plate rather than the Farallon which subducts beneath North America (Figure 5). The important difference is that the Kula plate's velocity with respect to North America was more northward, by about 30^{o}. This rotation of the basal tractions, especially during 85-60 Ma ago, causes systematic differences in the model results (Bird [8]). The Kula plate model actually gives a more accurate position for the Laramide band of shortening strains, and achieves a greater displacement of the mantle lithosphere, all the way to the Rio Grande Rift. However, it also predicts two large belts of strong clockwise rotations in addition to the rotated region in southern California. Since there is no hint of such features in the paleomagnetic literature, this model seems to be untenable. However, the question is important enough to warrant additional research.

In the rheologic set, it appeared that the solution given is reasonably unique, at least if one gives any weight to published rheologies of typical rocks obtained in the laboratory. In order to keep the Laramide shortening of Wyoming down to a reasonable value like 11%, it was necessary to assume a high coefficient of friction (0.85) in the crust. While much lower values have been proposed for the San Andreas Fault in California, they apparently do not apply to new faults of small displacement in the continental interior. Likewise, to keep the strain small it was necessary that the limit on the shear traction of the oceanic slabs should not be much greater than 27.5 MPa (which may be compared to 20 MPa of interplate traction in normal subduction (Bird [3]). In turn, this required the creep law of the mantle lithosphere to be reduced in strength to the lower bound of experimental determinations for olivine; it also required a large activation energy (**B** value) in the crust, to promote a weak detachment horizon. If these conditions were not met, then the relatively weak basal traction would not move the mantle lithosphere sufficiently, and the crustal thickening which should occur in the Rocky Mountain states would be found too far to the West. In short, every part of the rheology determined here lies at the outer limits of experimental determinations, so that there is no room for scaling or adjustment unless those determinations are flawed.

CONCLUSIONS

(1) The hypothesis that horizontal subduction caused the shortening of the Rocky Mountains is correct. The Rocky Mountain thrust- and reverse-faults formed in an environment of east-west to northeast-southwest compressive stress caused by the viscous coupling between the oceanic plate(s) and the base of the North American plate.

(2) The uplift of the central part of North America was also a consequence of horizontal subduction, which moved great volumes of lower crust from the coast to the interior.

(3) The heating of the crust of the Basin-and Range province was a consequence of the removal of the old North American mantle lithosphere by flat subduction (Figure 12). The mechanical energy for its extension was provided by the Pacific plate, acting across the San Andreas transform fault system.

(4) Computer model experiments may be used to determine the rheology of the North American and other continental plates.

ACKNOWLEDGEMENTS

This work was supported by the National Science Foundation through grants EAR 85-07665 and EAR 87-20468 to the University of California. Computing support in the form of matching time on the IBM 3090/VF was also provided by the University of California Los Angeles through its Office of Academic Computing. The frequent assistance of consultant Aeint de Boer in debugging and vectorizing the code was essential to the success of this project. Portions of this text appeared previously in Science (vol. 239, pp. 1501-1507).

REFERENCES

1. Atwater, T. (1970) Implications of plate tectonics for the Cenozoic tectonic evolution of western North America, **Geol. Soc. Am. Bull., 81**, 3513-3536.

2. Bird, P. (1978) Finite-element modeling of lithosphere deformation: The Zagros collision orogeny, **Tectonophysics, 50**, 307-336.

3, Bird, P. (1978) Stress and temperature in subduction shear zones: Tonga and Mariana, **Geophys. J. R. Astron. Soc., 55**, 411-434.

4. Bird, P. (1979) Continental delamination and the Colorado Plateau, **J. Geophys. Res.**, **84**, 7561-7571.

5. Bird, P. (1985) Laramide crustal thickening event in the Rocky Mountain foreland and Great Plains, **Tectonics, 3**, 741-758.

6. Bird, P. (1988) Formation of the Rocky Mountains, western United States: a continuum computer model, **Science, 239**, 1501-1507.

7. Bird, P. (1989) New finite element techniques for modeling deformation histories of continents with stratified temperature-dependent rheologies, **J. Geophys. Res., 94**, 3967-3990.

8. Bird, P. (1989) A test of competing "northern option" and "southern option" tectonic models for the Tertiary of North America, **Geol. Soc. Am. Abstr. Prog., 21**, 82.

9. Bird, P. (1991) Lateral extrusion of lower crust from under high topography, in the isostatic limit, **J. Geophys. Res.**, in press.

10. Bird, P., and J. Baumgardner (1981) Steady propagation of delamination events, **J. Geophys. Res., 86**, 4891-4903.

11. Bird, P., and J. Baumgardner (1984) Fault friction, regional stress, and crust-mantle coupling in southern California from finite element models, **J. Geophys. Res.**, **89**, 1932-1944.

12. Bird, P., and K. Piper (1980) Plane-stress finite-element models of tectonic flow in southern California, **Phys. Earth Planet. Int., 21**, 158-175.

13. Burchfiel, B. C., and G. A. Davis (1975) Nature and controls of Cordilleran orogenesis, western United States: extensions of an earlier synthesis, **Am. J. Sci., 275-A**, 363-396.

14. Cohen, S. C., and R. C. Morgan (1986) Intraplate deformation due to continental collisions: a numerical study of deformation in a thin viscous sheet, **Tectonophysics, 132**, 247-259.

15. Couples, G., and D. W. Stearns (1978) Analytical solutions applies to structures of the Rocky Mountains foreland on local and regional scales, in: V. Matthews, III (Ed.), Laramide Folding Associated with Basement Block Faulting in the Western United States, **Geol. Soc. Am. Mem., 151**, 313-335.

16. Cross, T. A. (1986) Tectonic controls of foreland basin subsidence and Laramide style deformation, western United States, **Spec. Publ. Int. Ass. Sediment., 8**, 15-39.

17. Cross, T. A., and R. H. Pilger (1978) Tectonic controls of Late Cretaceous sedimentation, western interior USA, **Nature (London) Phys. Sci., 274**, 653-657.

18. Davis, P. M., E. C. Parker, J. R. Evans, H. M. Iyer, and K. H. Olsen (1984) Teleseismic deep sounding of the velocity structure beneath the Rio Grande Rift, **N. M. Geol. Soc. Guideb., 35**, 29-38.

19. Dickinson, W. R., and W. S. Snyder (1978) Plate tectonics of the Laramide orogeny, in: V. Matthews, III (Ed.), Laramide Folding Associated with Basement Block Faulting in the Western United States, **Geol. Soc. Am. Mem., 151**, 355-366.

20. Engebretson, D. C., A. Cox, and R. G. Gordon (1985) Relative motion between oceanic and continental plates in the Pacific basin, **Geol. Soc. Am. Spec. Pap., 206**, 59 pp.

21. England, P. C., and G. A. Houseman (1985) The influence of lithosphere strength heterogeneities on the tectonics of Tibet and surrounding regions, **Nature (London) Phys. Sci., 315**, 297-301.

22. England, P. C., and G. Houseman (1986) Finite strain calculations of continental deformation 2: comparison with the India-Asia collision zone, **J. Geophys. Res., 91**, 3664-3676.

23. England, P. C., and M. Searle (1986) The Cretaceous-Tertiary deformation of the Lhasa block and its implications for crustal thickening in Tibet, **Tectonics, 5**, 1-14.

24. Gries, R. (1983) Oil and gas prospecting beneath Precambrian of foreland thrust plate in Rocky Mountains, **Am. Assoc. Pet. Geol. Bull., 67**, 1-28.

25. Grow, J. A., and C. O. Bowin (1975) Evidence for high-density crust and mantle beneath the Chile Trench due to the descending lithosphere, **J. Geophys. Res., 80**, 1449-1458.

26. Houseman, G., and P. C. England (1986) Finite strain calculations of continental deformation I: method and general results for convergent zones, **J. Geophys. Res., 91**, 3651-3663.

27. Houseman, G., D. P. McKenzie, and P. Molnar (1981) Convective instability of a thickened boundary layer and its relevance for the thermal evolution of continental convergent belts, **J. Geophys. Res., 86**, 6115-6132.

28. Ingersoll, R. V. (1982) Triple-junction instability as cause for late Cenozoic extension and fragmentation of the western United States, **Geology, 10**, 621-624.

29. Ingersoll, R. V., W. Cavazza, W. S. Baldridge, and M. Shafiqullah (1990) Cenozoic sedimentation and paleotectonics of north-central New Mexico: implications for initiation and evolution of the Rio Grande Rift, **Geol. Soc. Am. Bull., 102**, 1280-1296.

30. Longwell, C. R. (1945) The mechanics of orogeny, **Am. J. Sci., 243–A**, 417-447.

31. Mallory, W. W. (Ed.) (1972) Geologic Atlas of the Rocky Mountain Region, Rocky Mt. Assoc. Geol., Denver.

32. Mooney, W. D., L. W. Braile (1989) The seismic structure of the continental crust and upper mantle of North America, in: Bally, A. W. and A. R. Palmer (Ed.), The Geology of North America- An Overview, **The Geology of North America, A**, Geol. Soc. Am., Boulder, Colorado, 39-52.

33. Neugebauer, H. J. (1978) Crustal doming and the mechanism of rifting, part I: rift formation, **Tectonophysics, 45**, 159-186.

34. Parrish, D. K., A. Kriva, and N. Carter (1976) Finite element folds of similar geometry, **Tectonophysics, 32**, 183-207.

35. Sonder, L. J., P. C. England, B. P. Wernicke, and R. L. Christiansen (1987) A physical model for Cenozoic extension of western North America, in: Coward, M. P., J. F. Dewey, and P. L. Hancock (Ed.), Continental Extensional Tectonics, **Geol. Soc. Spec. Pub., 28**, 187-201.

36. Stephannson, O., and H. Berner (1971) The finite element method in tectonic processes, **Phys. Earth Planet. Int., 4**, 301-321.

37. Trimble, D. E. (1980) Cenozoic tectonic history of the Great Plains contrasted with that of the Southern Rocky Mountains: a synthesis, **Mt. Geol., 17**, 59-69.

38. Vilotte, J. P., M. Daignieres, and R. Madariaga (1982) Numerical modeling of intraplate deformation: simple mechanical models of continental collision, **J. Geophys. Res., 87**, 10709-10728.

39. Vilotte, J. P., M. Daignieres, R. Madariaga, and O. C. Zienkiewicz (1984) The role of a heterogeneous inclusion during continental collision, **Phys. Earth Planet. Int., 36**, 236-259.

40. Vilotte, J. P., R. Madariaga, M. Daignieres, and O. C. Zienkiewicz (1985) Numerical studies of continental collision: influence of buoyancy forces and an initial stiff inclusion, **Geophys. J. R. Astron. Soc.**, **84**, 279-310.

41. Wang, C.-Y., Y.-L. Shi, and W.-H. Zhou (1982a) On the tectonics of the Himalaya and the Tibet Plateau, **J. Geophys. Res.**, **87**, 2949-2957.

42. Wang, C.-Y., Y.-L. Shi, and W.-H. Zhou (1982b) The dynamic uplift of the Himalaya, **Nature (London) Phys. Sci.**, **298**, 553.

FIGURE CAPTIONS

Figure 1. Representation of a continental plate with two strong layers by two finite element grids. Left, a typical profile of strength (shear stress) as a function of depth. The middle crust and upper mantle are strong, but the lower crust is weak. Middle, typical profile of horizontal velocity when a shear traction is applied to the base of the continent; strong layers move as units, while weak layers are sheared. Right, oblique view of finite element grids representing the velocity fields of the layer tops. The grid properties are obtained from 3-D integrals, approximated numerically using selected vertical integrals at the Gauss points indicated by dots.

Figure 2. Cenozoic strain in west-central North America. Left, actual geology: Laramide shortening is represented by black areas showing exposures of Precambrian basement in uplifts. Later extension is represented by thin lines showing normal faults. At right, predictions of the continuum model. Contours are drawn on the common log of the greatest principal strain; the range is from 10^{-2} (1%) up to $10^{0.8}$ (600%). Small symbols show the character of the strain in terms of expected faults: black rectangles symbolize fault valleys produced by crustal extension; dumbbells symbolize trends of ranges and folds produced by crustal shortening; X patterns show orientations of strike-slip faults. (These symbols are all plotted at the same size for legibility, regardless of local strain.)

Figure 3. Cross-section from southwest to northeast across the western United States in the early Cenozoic, showing the horizontal subduction of the Farallon plate of ocean floor lithosphere. Oceanic crust (heavy black line) is only 5 km thick; continental crust (textured white) is initially 35-70 km thick. Volcanism occurs inland, where the Farallon plate bends downward, exposing hydrated oceanic crust to hot mantle asthenosphere (white regions). (This figure is to scale, including the curvature of the Earth.)

Figure 4. Grid of finite elements used to represent the crustal layer in this study. A similar layer (not shown) represents the mantle lithosphere of North America. Each layer has 609 nodes (circles) and 280 elements (isoparametric triangles). The grid is topologically rectangular for greatest computational efficiency. Northern, eastern, and southern edges were fixed; western edge is free; driving tractions were applied from below.

Figure 5. Reconstruction of plate shapes and positions for 65 million years ago, from Engebretson *et al*. [20]. As shown, the plate subducting beneath North America may have been either the Farallon or the Kula; both cases have been investigated.

Figure 6. Hingelines of the flat-subducting slabs beneath North America, from 90 to 30 million years ago, from Dickinson and Snyder [19]. West of the heavy line, North America overlies a moving oceanic slab of lithosphere. East of the line, it overlies hot, fluid asthenosphere. The positions of the lines are based on the shifting patterns of volcanism recorded in thousands of dated igneous rocks across the region.

Figure 7. Initial and final topography of the model. Left, assumed initial cordillera in British Columbia, Idaho, Nevada, Arizona, and Sonora at 85 million years ago. Right, predicted present topography. Contour interval 0.5 km = 500 m. Note that the Rocky Mountain region has been uplifted by as much as 2500 m.

Figure 8. Tectonics at the level of the North American mantle lithosphere. Left, horizontal velocity at 75 million years ago, during rapid flat subduction (not shown); velocity is contoured with interval of 1 cm/year. Right, final (present-day) predicted thickness of the old mantle lithosphere, contoured with 20 km interval. (The initial thickness was uniform at 70 km.) In the present Basin and Range province, the prediction is that no old mantle lithosphere remains, although a thin layer of new lithosphere would be reforming by cooling.

Figure 9. Initial and final thickness of continental crust in the model. Left, assumed initial cordillera in British Columbia, Idaho, Nevada, Arizona, and Sonora at 85 million years ago. Right, predicted present thickness of the crust. Contour interval 5 km. Note that the excess thickness of crust presently beneath the coastal cordillera is now beneath the Rocky Mountain region and western Great Plains.

Figure 10. Surface strain-rates at two times in the model. Left, 70 million years ago, during Laramide orogeny. Right, 10 million years ago, during Basin-and-Range extension. Contour interval 1×10^{-16}/s. Small symbols show the character of the strain-rate in terms of expected faulting: black rectangles symbolize fault valleys produced by crustal extension; dumbbells symbolize trends of ranges and folds produced by crustal shortening; X patterns show orientations of strike-slip faulting. (These symbols are all plotted at the same size for legibility, regardless of local strain-rate.)

Figure 11. Actual and predicted late Cenozoic rotations about a vertical axis. Left, closeup of southern California from Luydendyk *et al.* [31] identifies (shaded) regions that have undergone clockwise rotations averaging 90°. Right, model rotations, contoured with interval 10°; clockwise rotations are positive. The latitudes of the rotated regions are not well matched, and the model cannot resolve discrete blocks as in the actual case, so the correspondence may be fortuitous.

Figure 12. Summary of the proposed Cenozoic history of North America, shown in a West-East cross section (vertically exaggerated, and not to scale). Continental crust is white; mantle lithosphere is shaded; asthenosphere is white. In Mesozoic time, normal steep subduction built a coastal cordillera similar to the Andes. In Paleogene (early Cenozoic) time, flat subduction removed the lower crust and mantle lithosphere of North America northeastward into the interior. In Neogene (late Cenozoic) time, the subducting oceanic slabs fell away, leaving continental crust directly above hot asthenosphere (white regions).

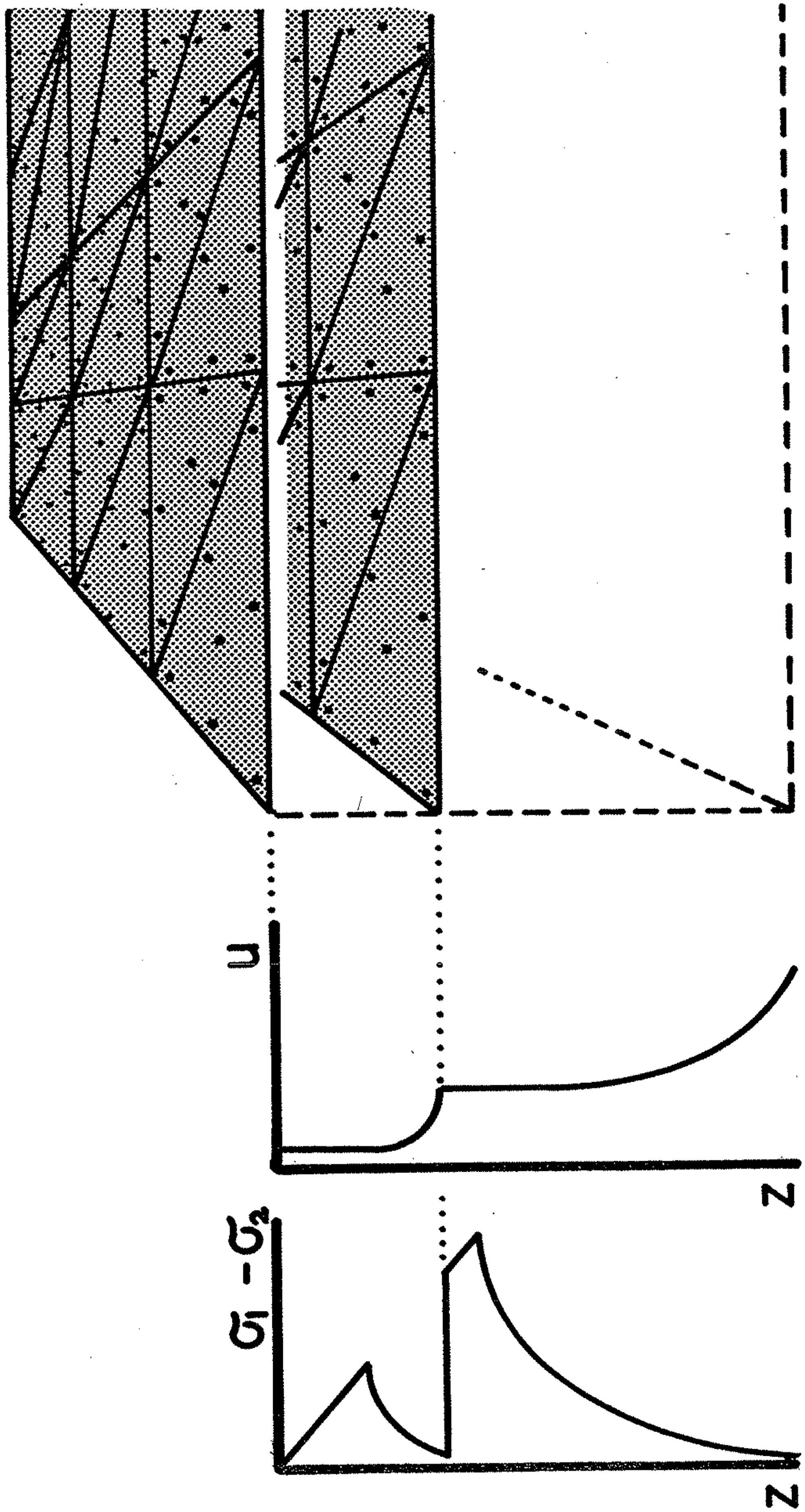
u
Z
σ1 - σ2
Z

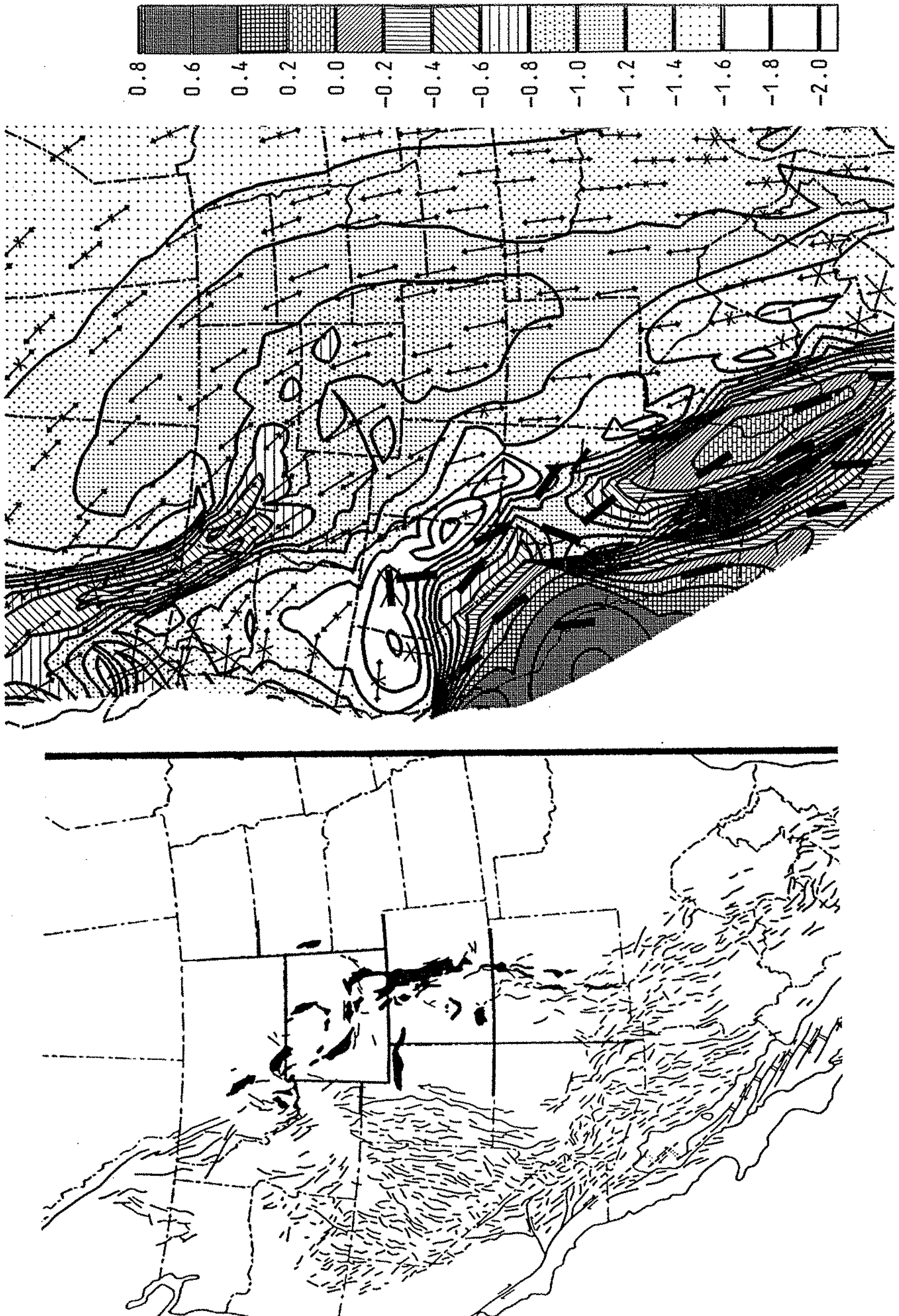

2

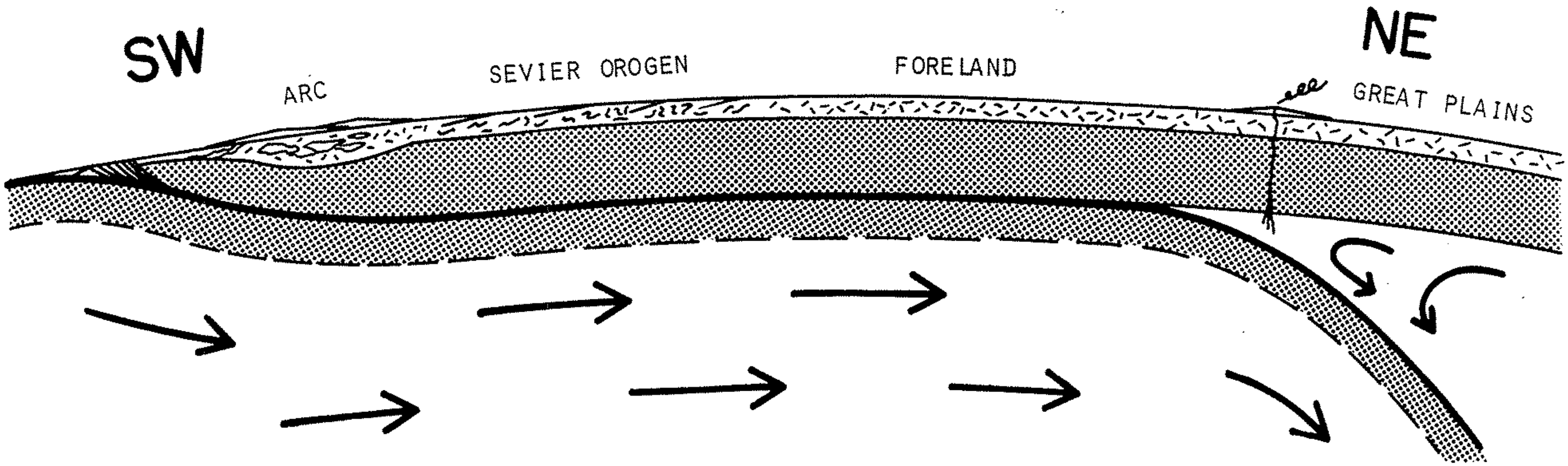
SW
ARC
SEVIER OROGEN
FORELAND
NE
GREAT PLAINS

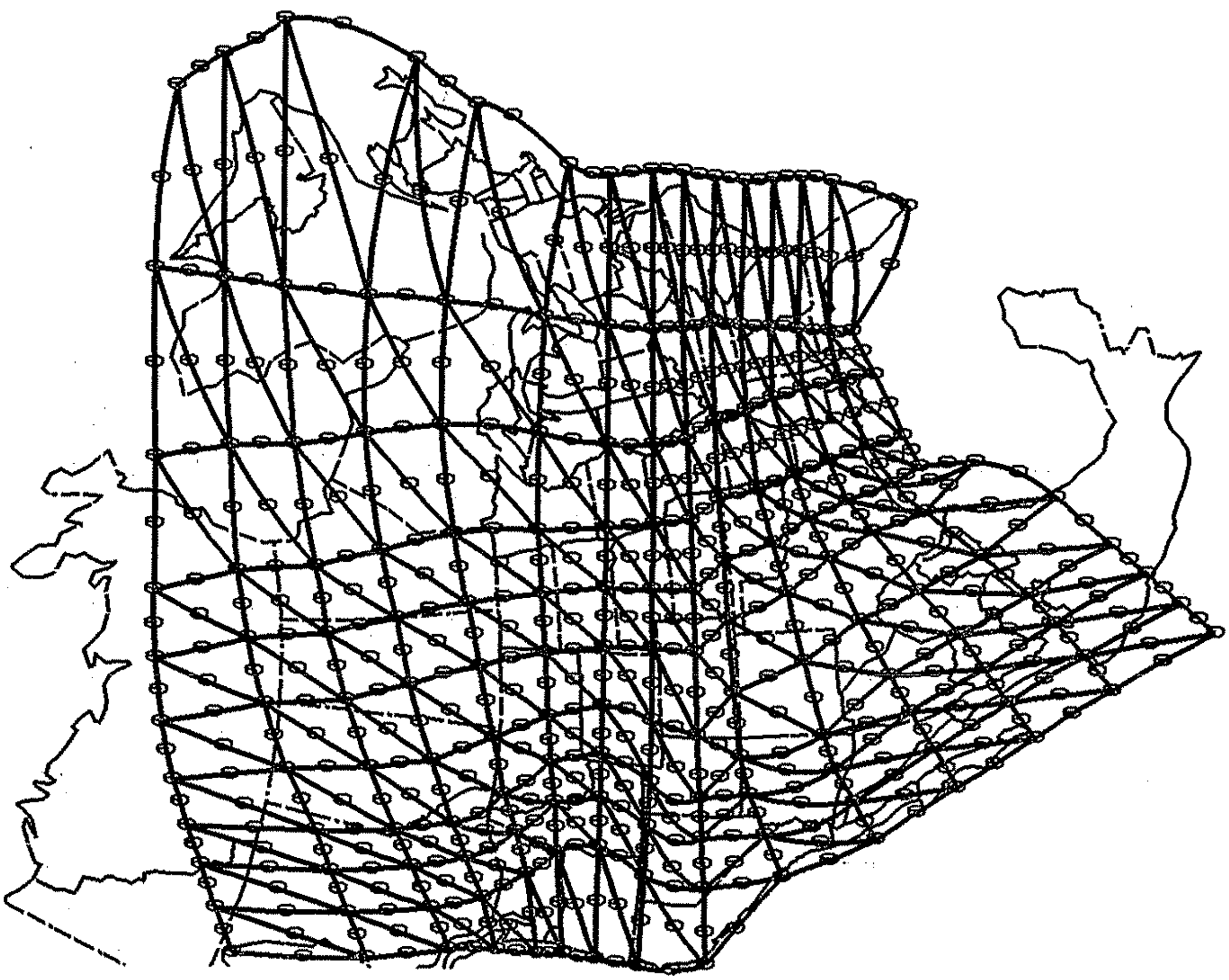

65 Ma (65-71)

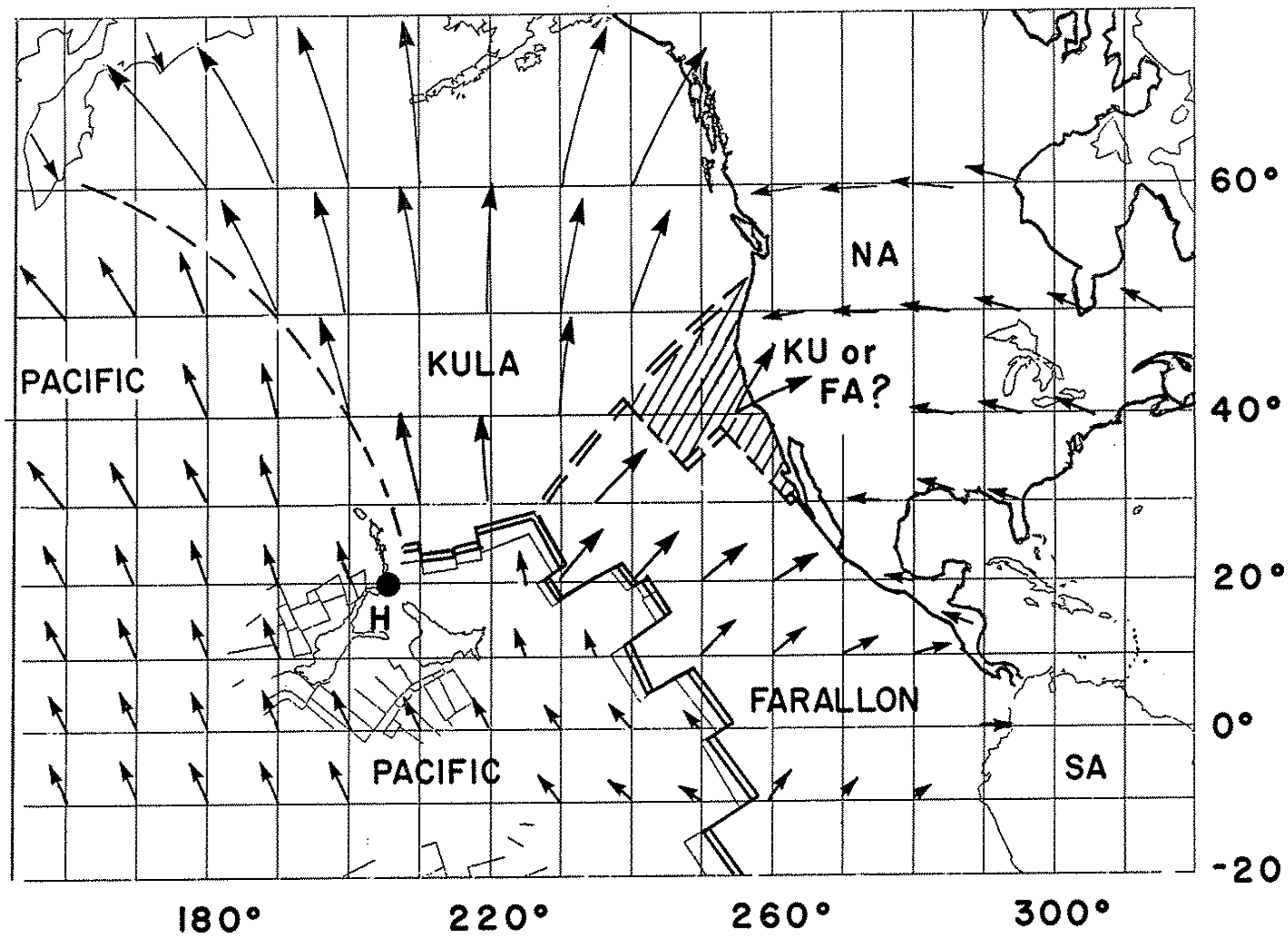
PACIFIC
KULA
NA
KU or
FA?
H
FARALLON
PACIFIC
SA
60°
40°
20°
0°
-20
180°
220°
260°
300°

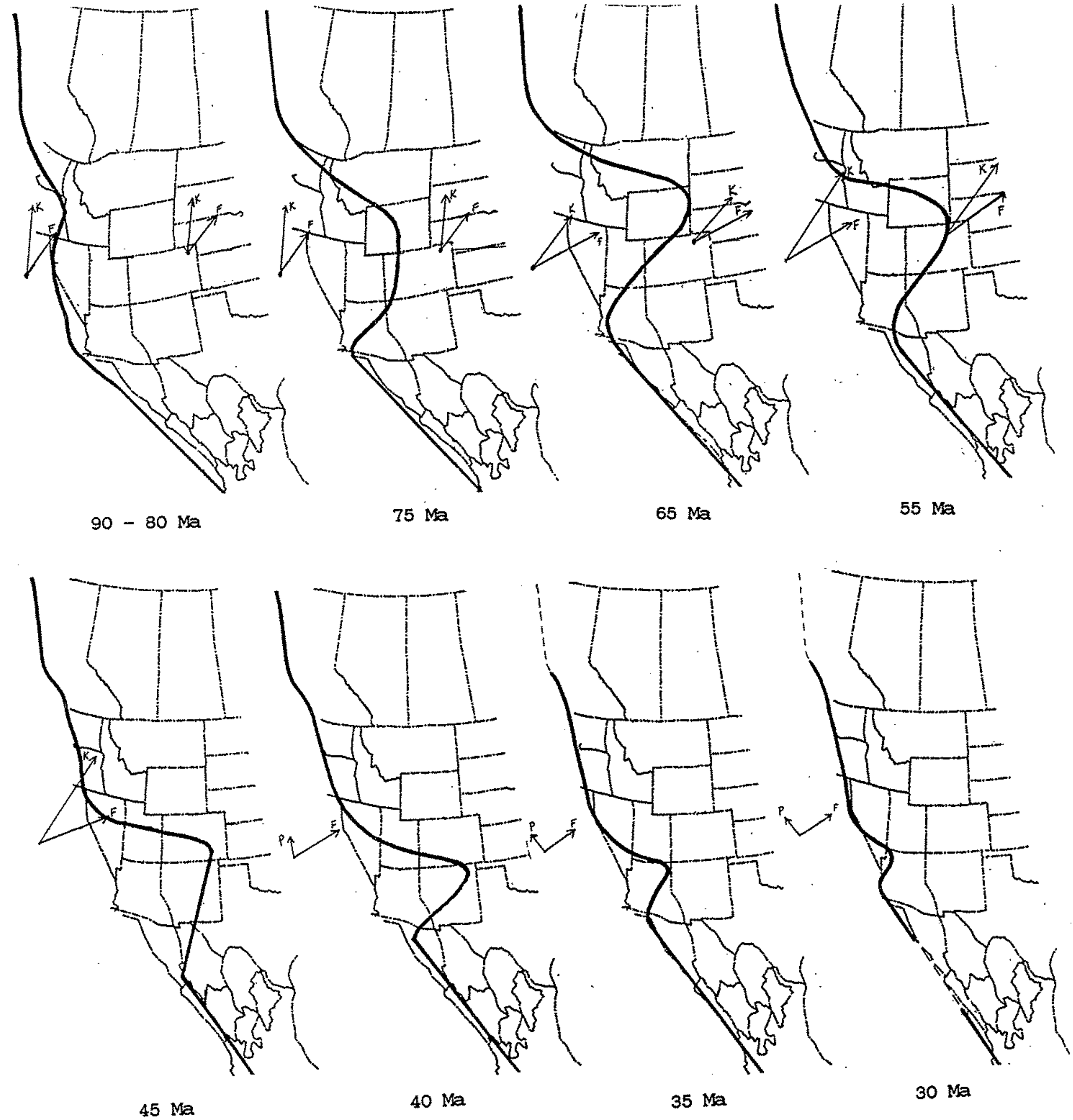
90 - 80 Ma
75 Ma
65 Ma
55 Ma
45 Ma
40 Ma
35 Ma
30 Ma

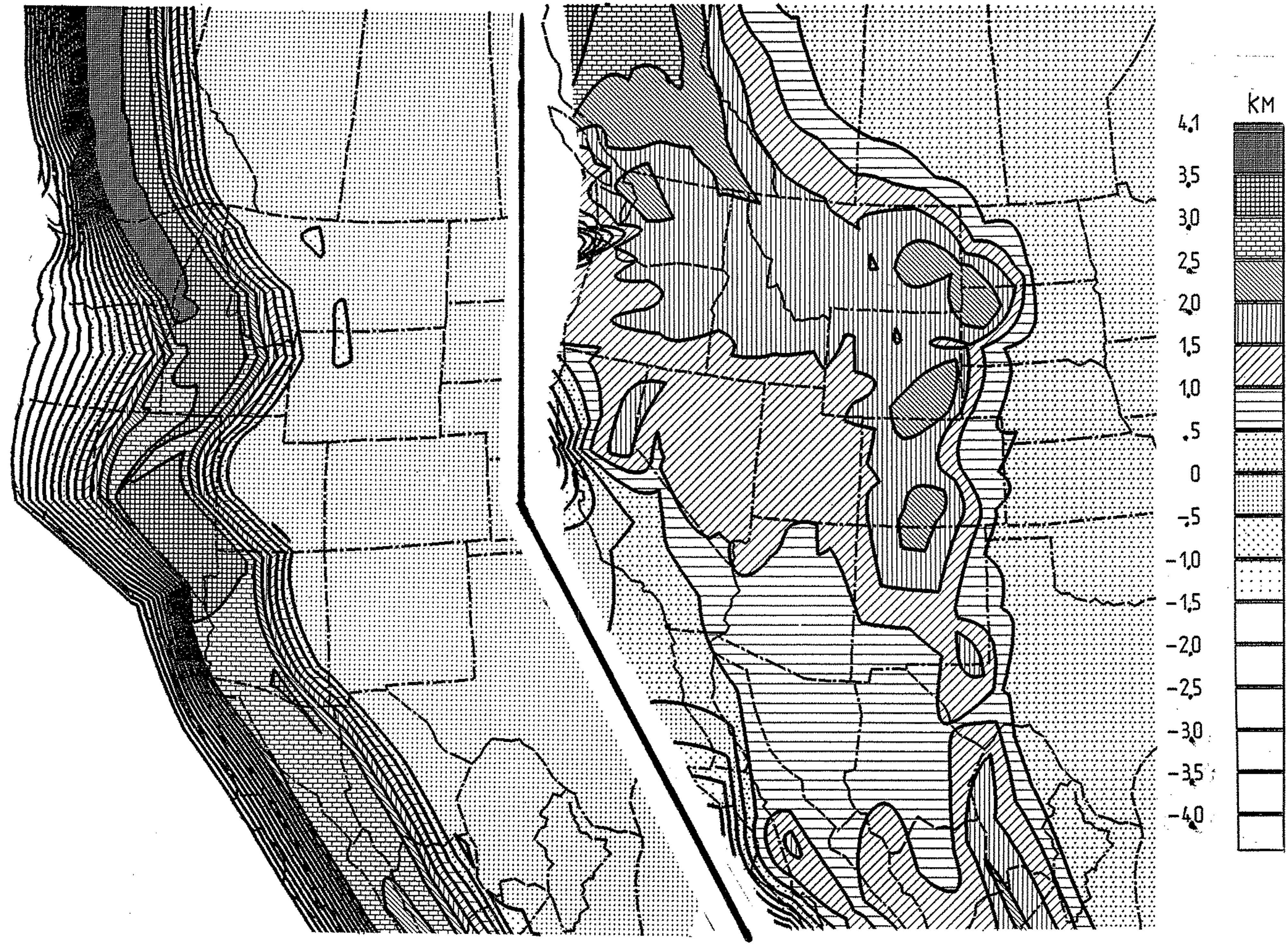
KM
4,1
3,5
3,0
2,5
2,0
1,5
1,0
,5
0
-,5
-1,0
-1,5
-2,0
-2,5
-3,0
-3,5
-4,0

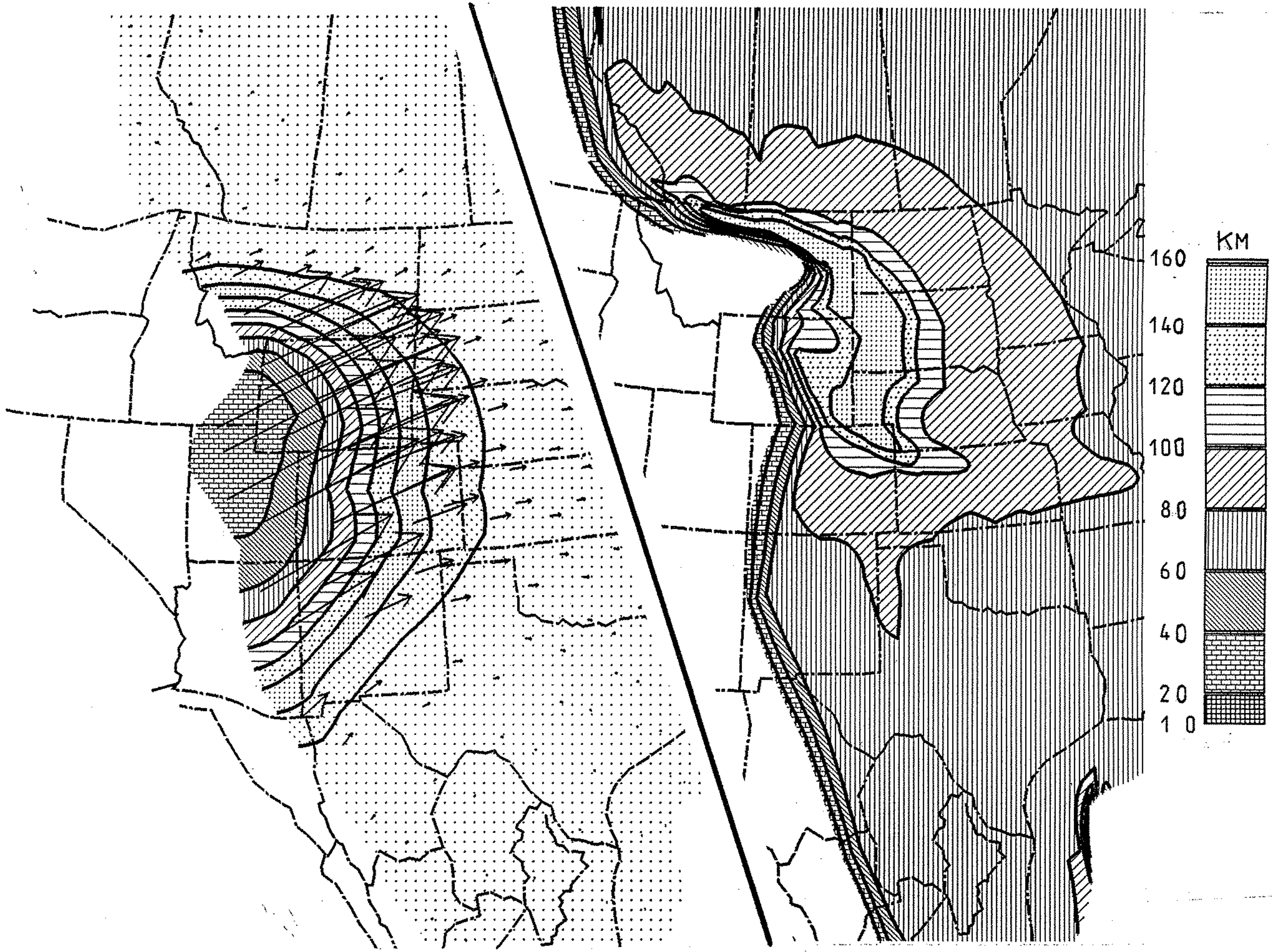
KM
160
140
120
100
80
60
40
20
10

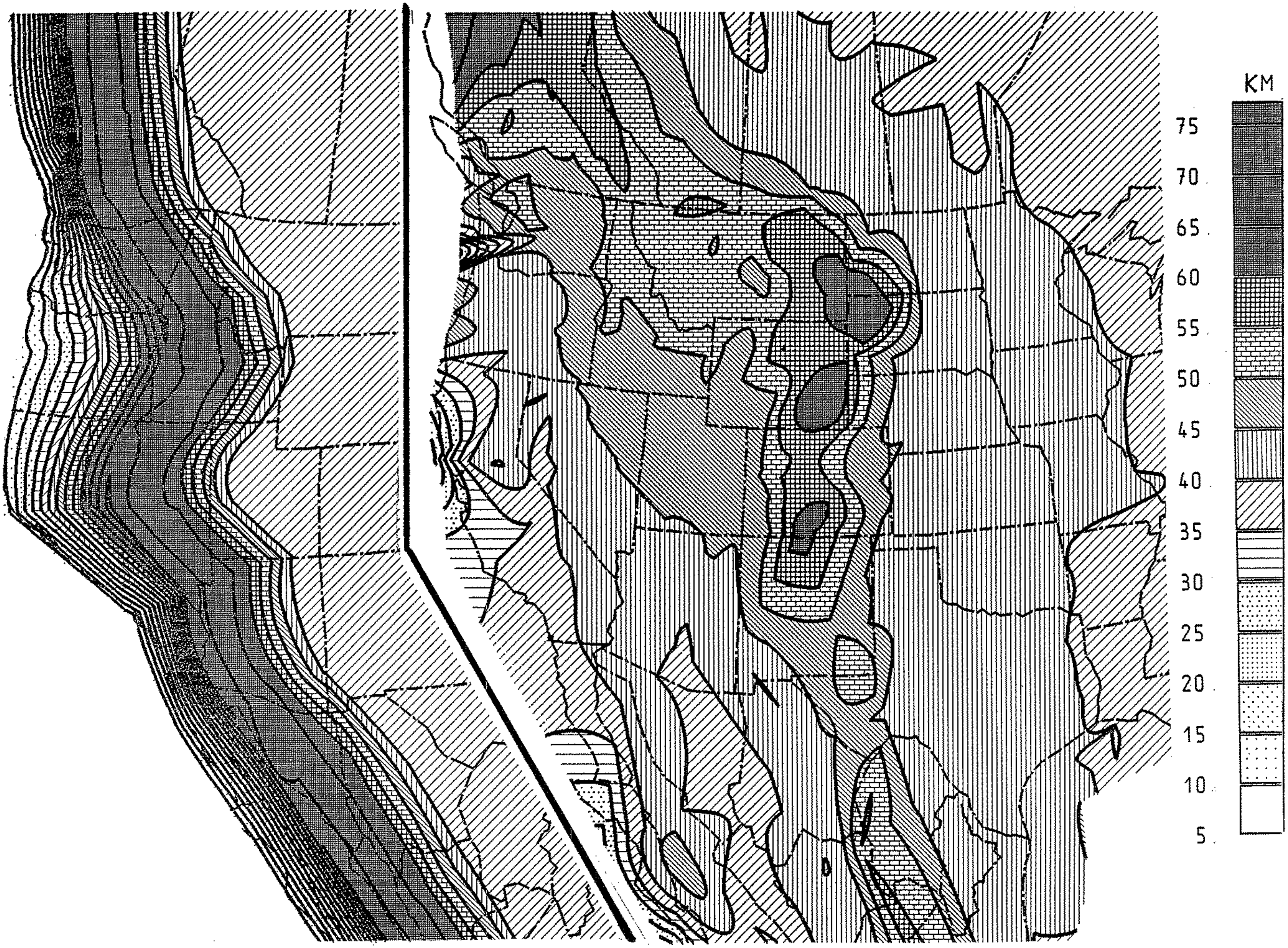
KM
75
70
65
60
55
50
45
40
35
30
25
20
15
10
5

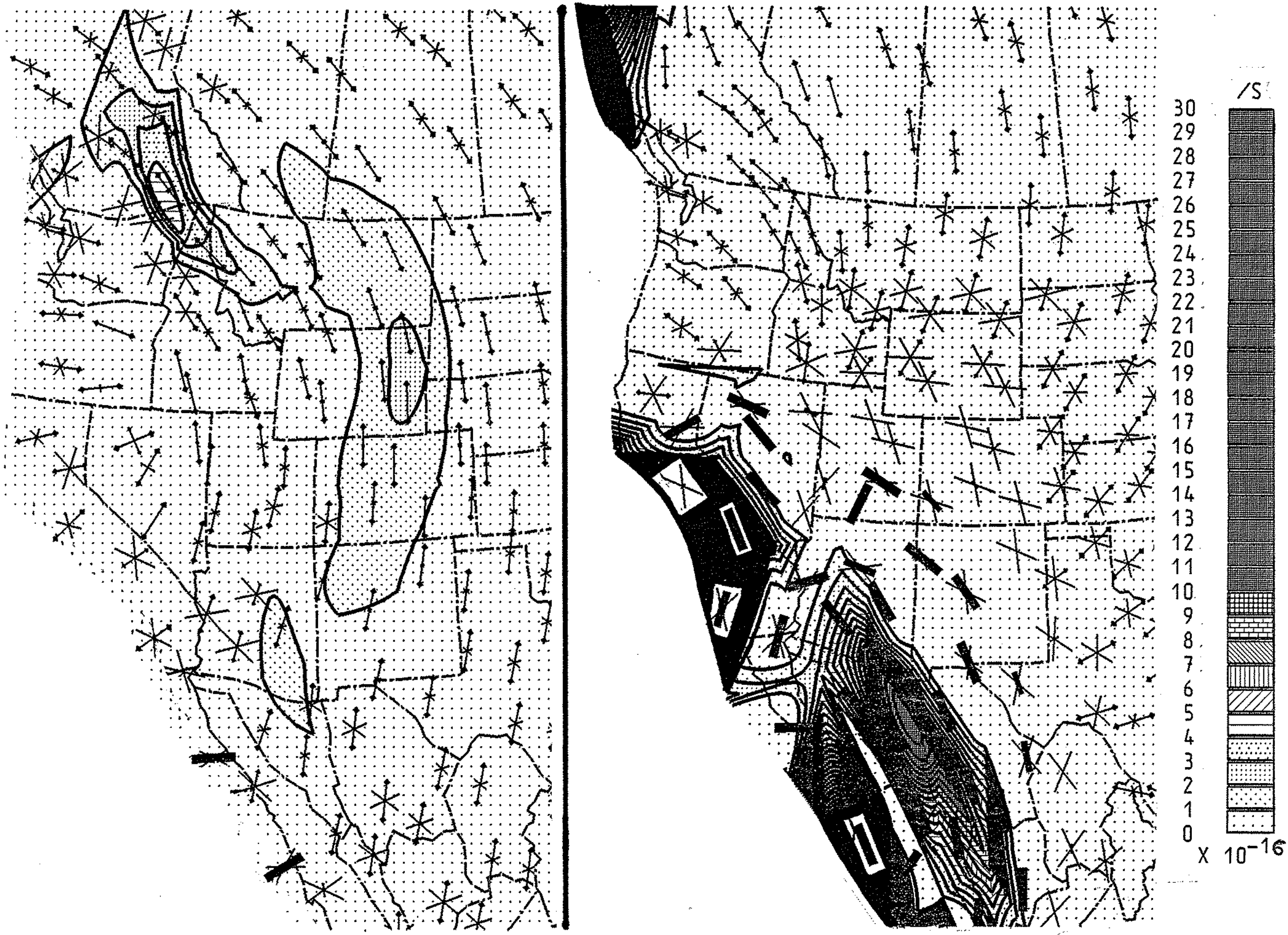
/S
30
29
28
27
26
25
24
23
22
21
20
19
18
17
16
15
14
13
12
11
10
9
8
7
6
5
4
3
2
1
0
X 10^{-16}

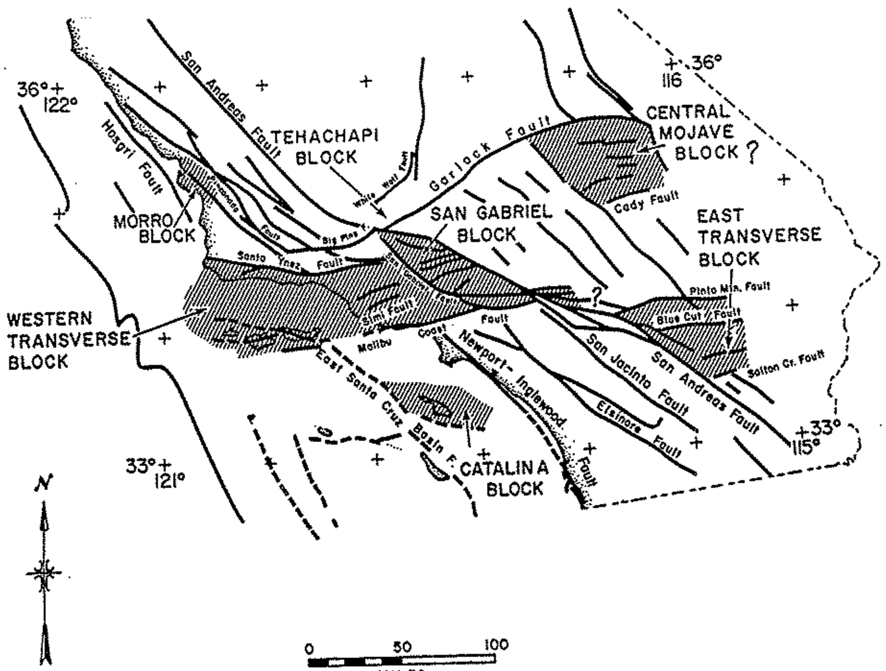

36°+ 122°
Hosgri Fault
San Andreas Fault
TEHACHAPI BLOCK
White Wolf Fault
Garlock Fault
+ 36° 116
CENTRAL MOJAVE BLOCK ?
MORRO BLOCK
Big Pine F.
SAN GABRIEL BLOCK
Cody Fault
EAST TRANSVERSE BLOCK
Santa Ynez Fault
Pinto Mtn. Fault
?
Blue Cut Fault
WESTERN TRANSVERSE BLOCK
Simi Fault
Malibu
Coast
Fault
Newport - Inglewood
Fault
San Jacinto Fault
San Andreas Fault
Salton Cr. Fault
East Santa Cruz Basin F.
Elsinore Fault
+33° 115°
33°+ 121°
CATALINA BLOCK
N
0 50 100
MILES

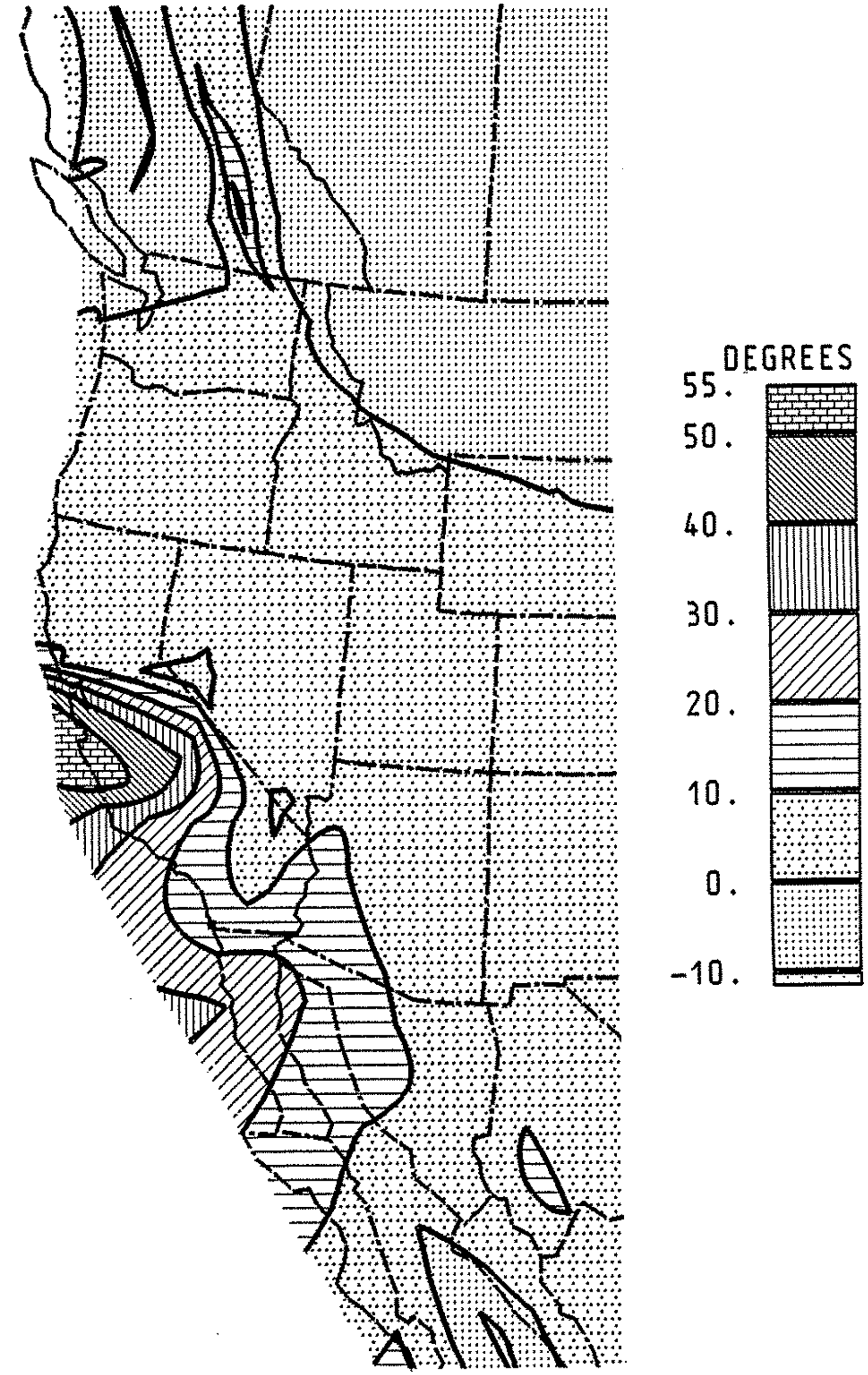

DEGREES
55.
50.
40.
30.
20.
10.
0.
-10.

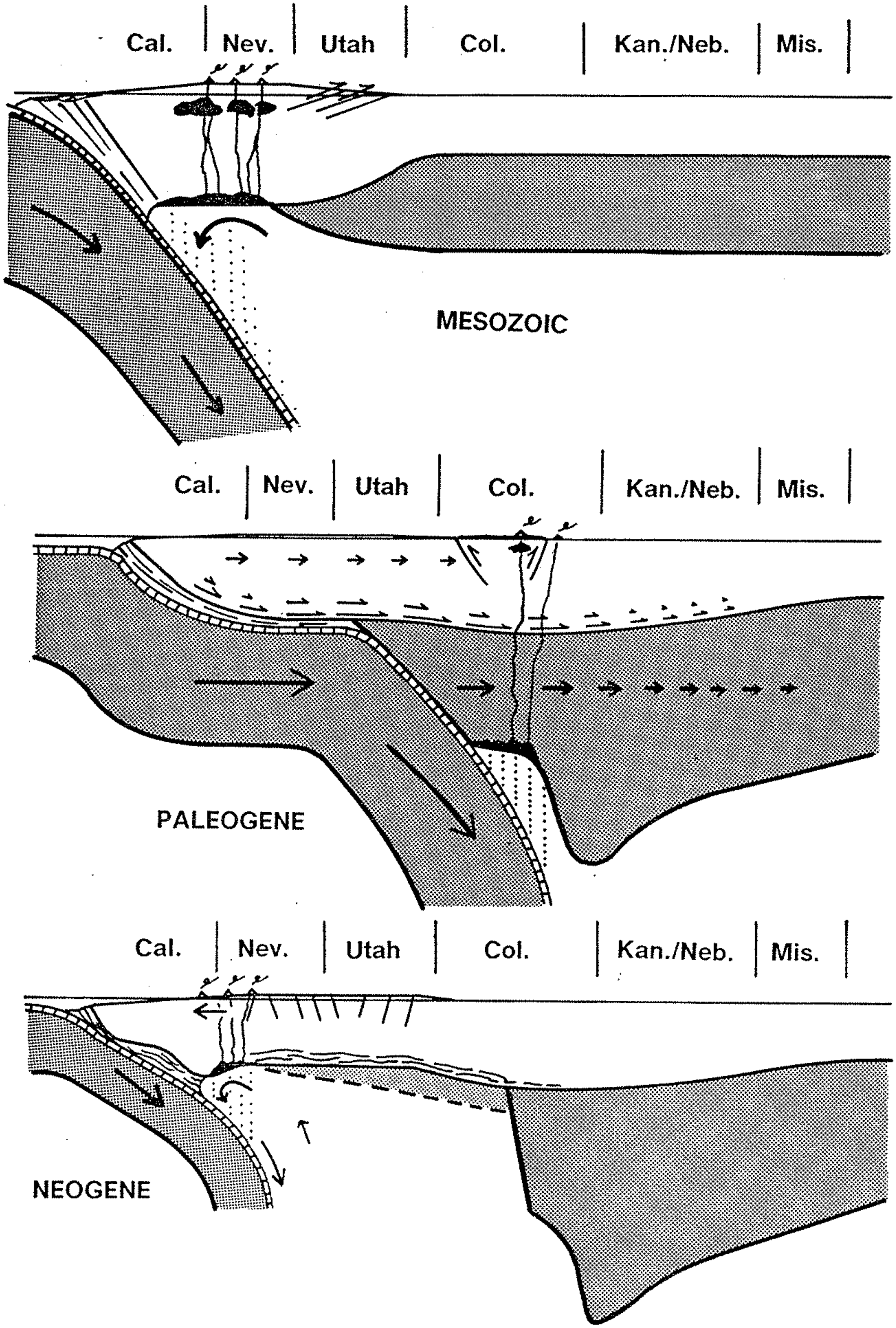
Cal.
Nev.
Utah
Col.
Kan./Neb.
Mis.
MESOZOIC
Cal.
Nev.
Utah
Col.
Kan./Neb.
Mis.
PALEOGENE
Cal.
Nev.
Utah
Col.
Kan./Neb.
Mis.
NEOGENE

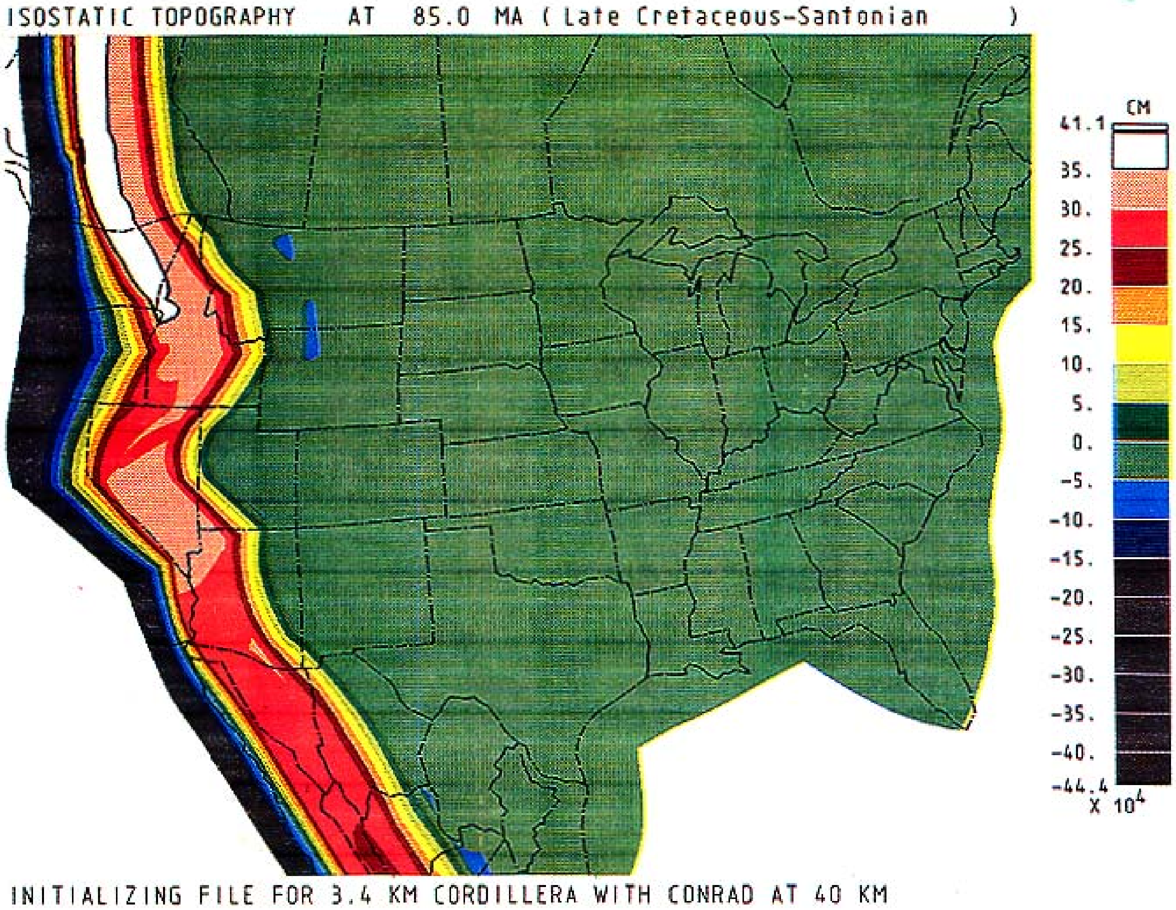
ISOSTATIC TOPOGRAPHY AT 85.0 MA (Late Cretaceous-Santonian)
CM
41.1
35.
30.
25.
20.
15.
10.
5.
0.
-5.
-10.
-15.
-20.
-25.
-30.
-35.
-40.
-44.4
X 10^4
INITIALIZING FILE FOR 3.4 KM CORDILLERA WITH CONRAD AT 40 KM

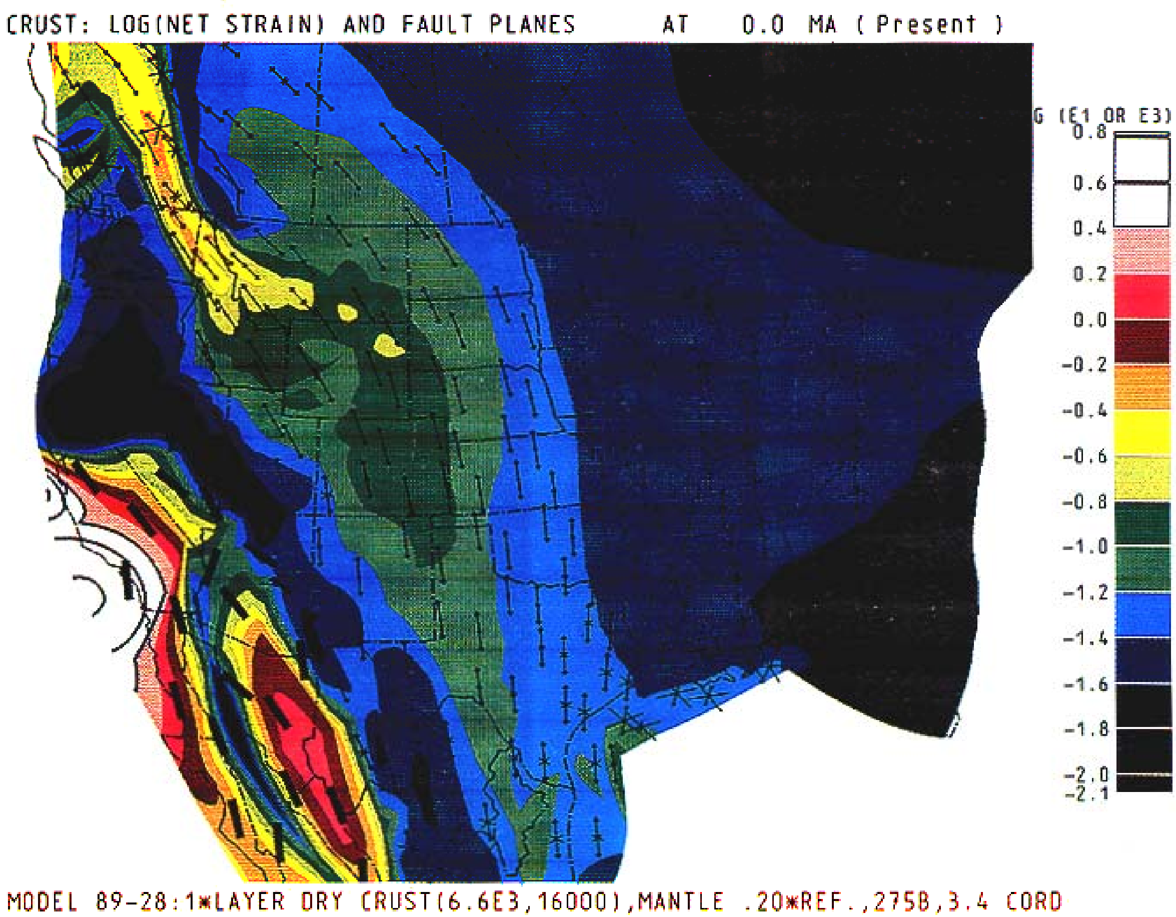
CRUST: LOG(NET STRAIN) AND FAULT PLANES AT 0.0 MA (Present)
G (E1 OR E3)
0.8
0.6
0.4
0.2
0.0
-0.2
-0.4
-0.6
-0.8
-1.0
-1.2
-1.4
-1.6
-1.8
-2.0
-2.1
MODEL 89-28:1*LAYER DRY CRUST(6.6E3,16000),MANTLE .20*REF.,275B,3.4 CORD

CRUST: NET CLOCKWISE ROTATION AT 0.0 MA (Present)

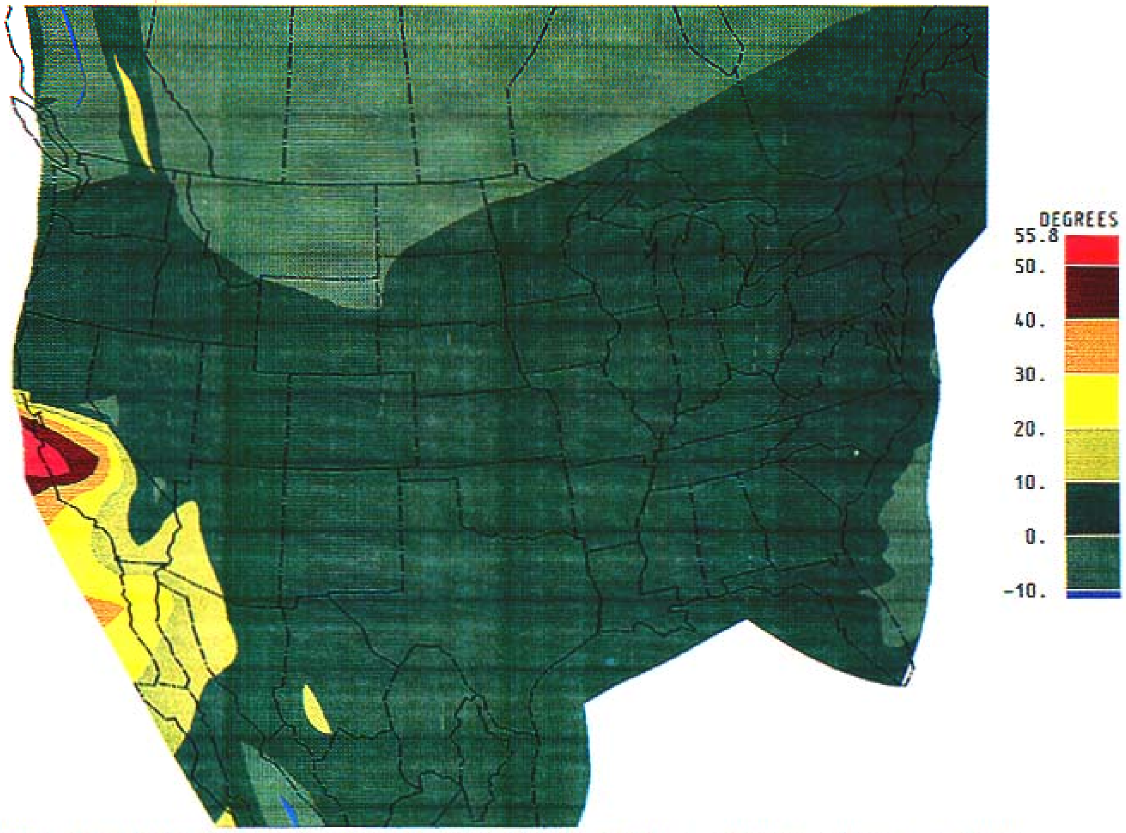

MODEL 89-28:1*LAYER DRY CRUST(6.6E3,16000),MANTLE .20*REF.,275B,3.4 CORD

TOPOGRAPHY AFTER DELAMINATION AT 0.0 MA (Present)

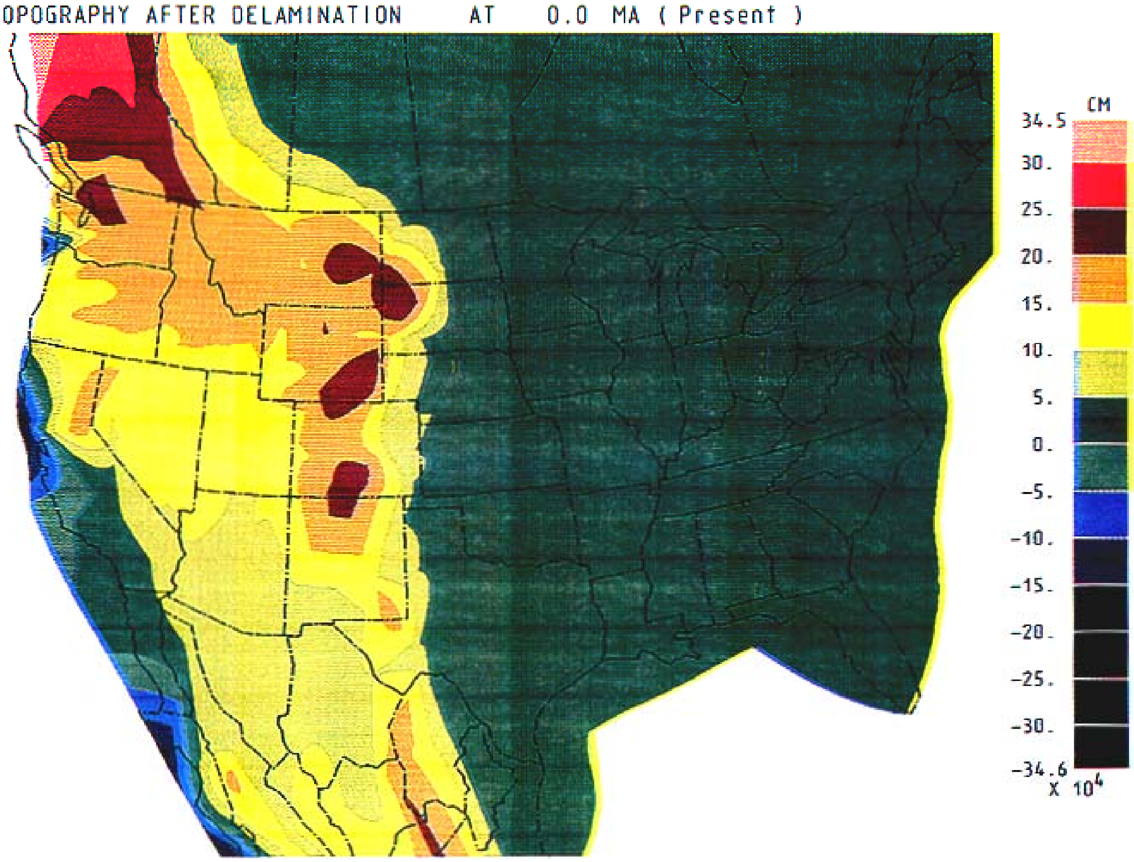

MODEL 89-28:1*LAYER DRY CRUST(6.6E3,16000),MANTLE .20*REF.,275B,3.4 CORD

Figures 32 (left), 27 (left), 36 (right), and 32 (right) from "Deformation and Uplift of North America in the Cenozoic Era," Peter Bird. (See page 67)